

ALMA MATER STUDIORUM - UNIVERSITÀ DI BOLOGNA

SCUOLA DI INGEGNERIA E ARCHITETTURA

DIPARTIMENTO DI INGEGNERIA INDUSTRIALE

CORSO DI LAUREA MAGISTRALE IN INGEGNERIA MECCANICA

TESI DI LAUREA
in
Meccanica dei Robot M

***DESIGN OF AN ACOUSTICALLY TRANSPARENT PRESSURE SENSOR FOR
BREAST ELASTOGRAPHY***

Candidato:

GIULIA AVALLONE

Relatore:

Chiar.mo Prof.
VINCENZO PARENTI CASTELLI

Correlatori:

dr. Françoise Siepel
Marcel Welleweerd

Marzo 2019

Sessione IV

Ai miei nonni
Maria e Augusto,
i primi a non mollare mai.

ABSTRACT

Breast cancer is the most commonly occurring cancer in women. Only in 2018 there were over 2 million new cases all over the world. The MURAB project, pursued at the University of Twente, has the aim of improving the breast biopsy procedure by reducing costs, patient discomfort and false negative rates. A 7-DOF KUKA robot arm steers an ultrasound transducer along a precise scanning trajectory to gather 3D volume image and stiffness values of the breast.

Elasticity is the property of a body to be deformed and differs between tumors tissue and soft tissue. Elastography is a non-invasive technique in which the elasticity of a tissue is determined. The aim of this study is to design an acoustically transparent pressure sensor, mounted on the tip of the ultrasound probe, that can measure pressure differences across its surface during the scan, and assess elastographic measurements. The main idea is to use a pad of a characterized material and sequentially ultrasound images able to visualize the section of the pad and evaluate its deformation during time. The transmission of ultrasound waves into a solid depends on the mechanical characteristics of the material and on its physic state. In this work the relations between the acoustic properties and the mechanical behavior of an acoustically transparent pad are studied and evaluated.

CONTENTS

- INTRODUCTION..... 1
 - Design constrains of the pressure sensor 3
 - Thesis outline..... 4
- 1. LITERATURE REVIEW 5
 - 1.1 ELASTOGRAPHY 5
 - 1.1.1 Theoretical basis of elasticity imaging 5
 - 1.1.2 Elasticity imaging methods..... 7
 - 1.2 ULTRASOUND 10
 - 1.2.1 Ultrasound interaction with matter 11
 - 1.2.2 Ultrasound image formation 15
 - 1.2.3 Ultrasound resolution..... 16
 - 1.2.4 Artifacts of ultrasound image 18
 - 1.2.5 Acoustical properties of some polymers..... 19
- 2. TACTILE PRESSURE SENSOR 21
 - 2.1 Capacitive soft sensors..... 22
 - 2.2 Sensor Performance 24
- 3. ULTRASOUND PRESSURE SENSOR 26
 - 3.1 Sensing modality..... 26
- 4. MATERIALS AND METHODS 30
 - 4.2 Pad manufacturing 30
 - 4.1 External set-up 33
 - 4.2 US images post-processing 35
 - 4.3 Arduino set-up 38
- 5. RESULTS..... 41
 - 5.1 Experiment: Calibration..... 41

5.2 Experiment: Deformation/Weight.....	41
5.3 Experiment: Pad deformation / Probe movement	44
CONCLUSIONS.....	46
BIBLIOGRAPHY	48

INTRODUCTION

The Global Cancer Observatory estimates that the top three cancers in term of incidence are lung, female breast and colorectal cancers. Among females, breast cancer is the leading cause of cancer death and only in 2018, over two million new cases all over the world were diagnosed [1]. The most important strategy to prevent deaths from breast cancer is early detection.

Considering that approximately 94% of cancerous lesions are potentially palpable, the more economic screening method is clinical breast exams (CBE). Professional clinicians palpate breast tissue to detect abnormalities in shape and stiffness. Recommendations for optimizing clinical performances are been implemented and, according to U.S. national screening program, CBE has reached a sensitivity of 58.8% and specificity of 93.4% [2]. To increment the effectiveness of breast screening, X-ray mammography was integrated in the cancer prevention program. Mammography is a medical imaging that detects modifications in intensity of an ionizing radiation that penetrate breast tissues. Cancers that exhibit a significantly difference of density than soft tissue, as calcifications, are easily detected by mammography. However, the sensitivity and specificity of mammography vary by different factors, such us age and position of the lesion, contributing to a consistent number of false-positive. Moreover Bleyer et al. [3] estimates that the frequency of overdiagnoses, that is the diagnosis and treatment of cancer that would have never caused symptoms during patient lifetime, is around 31% of all breast cancers. This, in addition to the fact that the exposition of X-ray has risks associated, have encouraged scientists to study alternative imaging modalities for breast screening. Women with a high cancer risk factor and with a dense breast for whom mammography is less sensitive, can use Magnetic Resonance Imaging (MRI) or Ultrasound Imaging (US) for early detection. MRI utilizes magnetic fields to distinguishes different tissues in the breast (fat, glandular, tissue, lesions, etc.) depending on the mobility of the hydrogen atoms in water and fat that contribute to differences in the signal creating MRI image [4]. It is been demonstrated that MRI, if added to mammography, provides a highly sensitive screening strategy [5]; it shows a superior capability in detecting ipsilateral and contralateral diseases and is the most sensitive method for detecting breast carcinoma. However, it has an imperfect specificity in recognizing benign and malignant lesions [6]. MRI is expensive, requires the injection of an intravenous contrast, it is time consuming and it is limited to the patients who cannot lay prone, are obese or have extremely large breast. Some of these disadvantages are improved upon ultrasound imaging, a real-time technique that uses pulses of high-frequency sound waves to detect specific characteristic of breast tissues composition. It is a safe and painless technology that is demonstrated to depict small, node-negative breast cancers not seen on mammography [7]. However, it is operator dependent and hence

hard to reproduce. The possible identification of abnormalities or suspicious lumps generally lead the clinician to recommend a biopsy, namely a removal of a tissue samples for examination under microscope. Biopsy is the only diagnostic procedure that can definitely determinate if the suspicious area is cancerous. The most widely used technique is the ultrasound guided percutaneous breast biopsy, in which a clinician places an ultrasound probe, used as visual feedback, over the site of the breast abnormality and guides a biopsy needle directly into the mass.

The goal of the MURAB project is to improve the precision and effectiveness in breast biopsy, using a 7-DOF KUKA robot arm that has to reach autonomously the best position for the needle insertion. Lesion targeting is performed thanks to the fusion of a single MRI image, that guarantees a high precision on the lesion localization, with the real time US imaging. It is been demonstrated that MRI-US fusion technology has diagnosed 30% more high-risk prostate cancer than a standard biopsy [8]. For this reason, MRI-US fusion is the visual servoing technique implemented in the control of the robot manipulator. This visual servo control technique allows the guidance of the robotic system thanks to the graphical representation of a confidence map regarding the intensity of each pixel of the US image. However, breast is made up of lobules, ducts and fatty and fibrous connective tissue. It is a dynamic system that changes shape and position with the application of external forces and physiological movements. Experiments have shown that it is very difficult to derive a generic relation between the pose of the probe with the confidence map created by the ultrasound image.

Simultaneous Localization And Mapping (SLAM) is the computational problem of knowing the robot's pose and simultaneously constructing a map of the environment. This spatial reconstruction is usually performed with visual inputs, but thanks to the increasing of spatial resolution and spatiotemporal response, tactile sensors have demonstrated the ability to serve as an "imaging" device [9]. Tactile sensing has been applied to grasp control, object recognition, modelling, exploration and tactile servoing [10]. For a safe and controlled robot-patient interaction, knowing the shape and the deformation of breast tissue is needed to assemble a more precise map of the environment.

A demonstrated method to detect soft tissue properties is Elastography. It is a medical imaging modality that uses MRI, US or mechanical measurements to map the elastic properties and stiffness of soft tissues. The first documented application is in breast mass evaluation [11]. In mechanical imaging (MI) the elasticity is detected from temporal and spatial changes in the skin stress pattern resulting from a sensor array pressed against the breast tissue [12]. It is demonstrated that malignant breast lesions increase hardness and strain hardening as well as decreased mobility in comparison with benign lesions. Differentiation capability of mechanical imaging is estimated to have an average sensitivity of 91.4% and a specificity of 86.8% [13]. Tactile sensing is earning more and more interest in the scientific world. A compliant capacitive sensor based on soft polymers and microfluidic electrodes is used to detect hard

lump in a phantom, obtaining a good estimation of cross-sectional area independent of embedding depth. This result underlines the possible utility of soft electronic sensors for application in medical imaging or clinical practices of palpation [14].

The goal of this thesis is to design a pressure sensor able to measure pressure differences across its surface during the US scan. It has to be mounted on the tip of the ultrasound probe without interfering with the sound waves propagation. For this reason, it has to be acoustically transparent, soft, stretchable and made of a material that is not harmful or irritable for the human skin. Knowing the pressure distribution on its surface permits to assess medical information about the breast, and simultaneously to have additional data for the robot control.

The main purpose is that the robot must be equipped with different sensing modalities to be able to operate in human dynamics environments. The information provided by the combination of different sensing modality may reduce the uncertainty and increase the accuracy of the local pose of the probe. Moreover, knowing the distribution of pressures on the US probe allows to have an elastography assessment of the breast and to control the correct contact with the skin.

Design constraints of the pressure sensor

First of all, it is necessary to underline the project constraints to follow in the design of the pressure sensor. It is a medical device, so it has to be competent for the medical environment, namely that do not have to influence other medical instruments and has to be safe for the patients and clinicians. In accordance with medical regulation it has to be mountable and sterilizable or disposable. The sterilization solution is preferable for a low production of waste; thus the pressure sensor has to be made of a material that can be chemically treated with the most common cleaning processes, such as steam sterilization, dry heat sterilization and chemical or radiation sterilization. In order to be part of a robot system that autonomously proceed with the breast scanning, the pressure sensor has to be fixable to the ultrasound probe without interfering the correct use of the ultrasound instrument. Thus, it has to be acoustically transparent and do not have to influence the ultrasound wave penetration coming from the transducer. As it is described in the chapter 2.2, the ultrasound transparency depends on several factors, but it is mainly correlated with the attenuation coefficient and the acoustic impedance of the materials involved. The attenuation coefficient describes the reduction of sound wave amplitude during the propagation along the material. It is strongly associated with the thickness of the material; increasing the depth of the material causes a major attenuation effect. The acoustic impedance defines the angle of refraction of the sound waves when encounter a tissue boundary and consequently determines the image pixels intensity correspondent to that boundary. In order to have the maximum intensity in the breast tissue, it is necessary to have the minimum loss of signal in the pressure sensor. This can be reach using

a pressure sensor made of a thin layer of a material that shows a low attenuation coefficient, and a value of acoustic impedance that guarantees the minimum refraction index possible. It happens when the acoustic impedance coefficients of the boundary materials are similar. Thus, the material of the pressure sensor has to show an acoustic impedance similar to the skin one. Moreover, the sensor material must be not harmful or irritable for the human skin.

Thesis outline

The first chapter of this thesis includes the literature review and it is divided into two sections. In the first one, some elastographic methods are described. Elastography is a medical technique thanks to which it is possible to assign mechanical behaviour, such as the elastic modulus, to soft tissues. It is a useful method because it permits to characterize different tissue type inside the body, incrementing the probability of early detection of abnormalities. The second section describes the ultrasound machines with a focus on the physics of the ultrasound waves and some acoustic properties. Furthermore, the methodology of medical ultrasound image formation is described, which is possible only with the introduction of some assumptions that simplify the physics of the system. These simplifications implicate the presence of errors in the ultrasound image and are referred as image artifacts. The second chapter describes the use of soft tactile sensors as a solution to the problem described. However, only a theoretical study is introduced. The third chapter described the solution promoted by the University of Twente and the subsequent chapters contain the experiments made to test the pressure sensor.

1. LITERATURE REVIEW

1.1 ELASTOGRAPHY

Elastography is a technique in which the elasticity of a soft tissue is assessed during the application of a mechanical compression or vibration. Elastography imaging techniques have received a growing attention in recent years; it is a non-invasive technique able to detect difference of tissue stiffness in liver, breast, thyroid, kidney and prostate. To fulfill the commercial requirements and to be competitive in the clinical market, these techniques are implemented in the traditional detection and visual technologies. For example, Ultrasound Elastography (USE), that is performed with an ultrasound probe, has been introduced into clinical routine for specific applications such as liver fibrosis assessment or breast lesion characterization [21]. Another commercial device uses an array of pressure sensor to detect the pressure distribution and the relative stiffness in breast. This technique is called Mechanical Imaging (MI).

1.1.1 Theoretical basis of elasticity imaging

The evaluation of soft tissue properties is a complex and difficult issue. In general, soft tissue are anisotropic, viscoelastic and non-linear. However, in order to reduce the complexity of the mathematical resolution, elastographic techniques are often based on modeling tissue as a linearly viscoelastic, incompressible and isotropic medium.

The general linear equation of dynamic equilibrium describing the motion of a mechanical body in Cartesian coordinates is [11]:

$$\sum_{j=1}^3 \frac{\partial \sigma_{ij}}{\partial x_j} + f_i = \rho \frac{\partial^2 u_i}{\partial t^2} \quad (1.1)$$

where σ_{ij} are the components of stress tensor, u_i represent the displacement vector and f_i is the body force per unit volume acting on the body in the x_i direction, t is time and ρ is the density of the material. The stress tensor of an elastic material can be written in the form [21]:

$$\sigma = c \varepsilon \quad (1.2)$$

where c is a fourth-order tensor called stiffness tensor or elasticity tensor and represent the intrinsic properties of the material. Assuming that soft tissue is an isotropic material means that the elastic properties are independent of the orientation of the axes with a consequently reduction of the number of

elastic constants into the stiffness tensor. The elastic properties may be expressed using only two parameters, called Lamè constants and indicated as λ and η . So, the stress tensor can be expressed [22]:

$$\sigma_{ij} = \lambda \Theta \delta_{ij} + 2\mu \varepsilon_{ij} + \xi \frac{\partial \Theta}{\partial t} \delta_{ij} + 2\eta \frac{\partial \varepsilon_{ij}}{\partial t} \quad (1.3)$$

where δ_{ij} is the Kronecker delta, a function that is one if the variables i and j are equal, and zero otherwise. The first two terms of the equation describe the elastic behavior and the last two terms the damping of the mechanical body. If the body is deformed very slowly to the final position, only static deformation needs to be considered and the last two terms vanish. Θ is the divergence of the displacement vector [11]:

$$\Theta = \nabla \cdot \mathbf{u} = \frac{\partial u_1}{\partial x_1} + \frac{\partial u_2}{\partial x_2} + \frac{\partial u_3}{\partial x_3} = \varepsilon_{11} + \varepsilon_{22} + \varepsilon_{33} \quad (1.4)$$

$$\varepsilon_{ij} = \frac{1}{2} \left(\frac{\partial u_i}{\partial x_j} + \frac{\partial u_j}{\partial x_i} \right) \quad (1.5)$$

The expression of linear elasticity can be further simplified by assuming that soft tissue is incompressible. This means that the volume changes due to deformation only and mathematically it is expressed with the Poisson's ratio equal to 0.5 and the term Θ equal to zero. Similarly, if the material volume does not change, the longitudinal Lamé constant λ approaches infinity. Thus, the stress tensor can be written [11]:

$$\sigma_{ij} = p \delta_{ij} + 2\mu \varepsilon_{ij} \quad (1.6)$$

Where p is the static internal pressure, defined as [11]:

$$p = \lim_{\substack{\lambda \rightarrow \infty \\ \mu \rightarrow \infty, \Theta \rightarrow 0}} \lambda \Theta \quad (1.7)$$

The elastic component of stress-strain relation is written in terms of the Lamé coefficients, but other more common elastic moduli can be derived from these parameters, such as Young's modulus E and the Poisson's ratio ν , that is equal to 0.5 [11].

$$\mu = \frac{E}{2(1 + \nu)} = \frac{E}{3} \quad (1.8)$$

$$\lambda = \frac{E \nu}{(1 + \nu)(1 - 2\nu)} \rightarrow \infty \quad (1.9)$$

Therefore, deformation of an incompressible medium can be completely characterized by a single material parameter μ [23]. Combining all these equations, the problem is formulated as a system of four equations containing three components of displacement vector $u_i(x_1, x_2, x_3)$ and three component of unknown pressure $p(x_1, x_2, x_3)$. The system as defined, has an infinite number of solutions. The unique solution is determined by the boundary conditions that can be expressed in terms of displacements or stress on the surface of the object. By solving this system, the displacement field is obtained and used to calculate the strain tensor and the value of $\mu(x_1, x_2, x_3)$. Elasticity imaging is the reconstruction of the spatial distribution of the Young's modulus $E(x_1, x_2, x_3)$, that is strictly related to the distribution of $\mu(x_1, x_2, x_3)$.

However, in direct reconstruction methods, it is difficult to obtain strong boundary conditions and solve the inverse problem for an arbitrary geometry and elasticity distribution. Usually, the unknown elasticity modulus can be estimated with numerical algorithm that minimize the error function between the measured displacement or strain distribution and the theoretically predicted data [11].

1.1.2 Elasticity imaging methods

In the last years several studies have demonstrated different methods to perform elasticity imaging with different physical principles, such as ultrasound, MRI, mechanical pressure sensing, X-Ray, optical and acoustic signal. All these methods have in common two elements: a force or stress is applied to a tissue and the mechanical response is detected. The force, for example a mechanical excitation or an ultrasound radiation, generates a variation of characteristic parameters over time that are elaborated to differentiate the stiffness between close tissues. The methods most used and studied are Ultrasound Elastography and Mechanical Elastography.

Ultrasound Elastography

There are two types of ultrasound elastography, strain elastography (SE) and shear wave elastography (SWE). Both evaluate difference of the rate at which the ultrasound wave propagates after an external stimulus. The wave velocity varies from one medium to another, depending on the elastic properties of the material, density and compressibility of the medium. A simplified equation that describes wave velocity may be written as:

$$v = \sqrt{\frac{c}{\rho}} \quad (1.10)$$

where ρ is density and \mathcal{C} is the stiffness characteristic matrix of the medium. There are two types of wave propagation in ultrasound: if the direction of displacement of medium particles is the same as the direction of oscillation of the source of ultrasound, the waves are called longitudinal waves. When the propagation direction is perpendicular to the source one, the waves are referred as transverse or shear waves [20]. Considering separately the directions of wave propagation, the stiffness matrix can be reduced to two parameters that are commonly used to characterize the mechanical properties of solid materials: the bulk modulus K for longitudinal waves, and the shear modulus G for shear waves [21].

$$K = \frac{E}{3(1 - 2\nu)} \quad (1.11)$$

$$G = \frac{E}{2(1 + \nu)} \quad (1.12)$$

Assuming the Poisson ratio equal to 0.5, it is possible to correlate the shear wave speed (c_s) with the Young modulus E [21].

$$E = 3G = 3\rho c_s^2 \quad (1.13)$$

Shear wave elastography (SWE) is a quantitative technique in which the stiffness value is displayed as the velocity of the shear waves: differences in the wave velocity are read into differences in elastic modulus, thus is possible to differentiate tissues. There are currently three technical approaches for this method that differ in the signal processing. The main characteristic is that a tissue portion is located using an ultrasound probe that is able to detect the propagation of shear waves generated by a controlled vibrating device that is pressed on the body surface. Some examples of commercially available device are Fibroscan™ probe, Virtual Touch™ Quantification by Siemens available since 2008 and the Elast-PQ™ by Philips introduced in 2013. [21]

Strain Elastography (SE) evaluates how a tissue changes when a normal force is applied to it. A set of digitized radio-frequency echo lines are acquired before and after the external stimulus. Congruent echo lines are subdivided into small temporal windows and compared; changes in arrival time of the echoes before and after compression are estimated and associated to a tissue displacement and consequently to the strain. However, the applied stress is not numerically quantifiable, and the Young's modulus is only measured qualitatively and displayed as a semitransparent color map overlaid on the B-mode image. Typically, it is used a pseudo-quantitative measurement called strain ratio, which is the ratio of strain measured in a reference tissue region to strain measured in the target lesion. A strain ratio higher than one indicates lower strain and greater stiffness [21].

It's been demonstrated that the addition of Ultrasound Elastography to the standard breast ultrasound screening and diagnostic, can be performed in few minutes and guarantee higher sensitivity and specificity in the characterization of breast lesions. Guidelines by the EFSUMB (European Federation Societies for Ultrasound in Medicine and Biology) recommends the implementation of these technologies in the present methodology for breast cancer detection. [24]

Mechanical Elastography

Mechanical elastography is an imaging technique that evaluates elasticity of a tissue by measuring skin stress patterns thanks to a force sensor array pressed against the tissue [13]. The mechanical imaging probe acts like a human fingertip during clinical examination and detect the internal structure of a tissue thanks to the evaluation of temporal and spatial changes in stress patterns. The stress data are gathered into a two-dimensional or three-dimensional image that visually shows the internal soft tissue structure. Lesions in soft tissue are characterized by an increased hardness [13] and, since pressure distribution detected depends on the Young's modulus, it is possible to localize and recognize differences in the mechanical characteristic between normal tissues and lesions. Egorov et al. [12] claim that, for practical purposes, the Elastic Modulus can be evaluated with a linear expression that considers the pressure values at specific locations at the edges of the sensor array:

$$E_0 = \frac{a \cdot P_c}{P_s + b} \quad (1.14)$$

where P_c and P_s are the pressure values and a and b are constants. A current available medical device that uses this technology is produced by Sure, inc under the trade name of SureTouch. The probe head measures 50 mm in length and 40 mm in width and is made of an array that comprises 192 (16 x 12) capacitive pressure sensors. This approach utilizes sensing devices that are many orders of magnitude stiffer than body tissues. A future study work is to understand if mechanical imaging techniques based on softer sensor, as soft tactile sensor, could facilitate and improve the evaluation of curved, hard and heterogeneous soft tissues [14].

Another experimental approach is the **Acousto-Mechanical Imaging (AMI)** that has the ambitious to detect the mechanical properties of a tissue via the synergy of the surface stress pattern measured by a force sensor array and the internal strain obtained by strain elastography [36]. It should fuse the qualities of the two sensing modality permitting to extend the range of manual breast examination with the detection of impalpable lesions.

1.2 ULTRASOUND

Ultrasound in medical diagnosis, is an imaging technique that uses sound wave with a frequency higher than 20 kHz, to visualize organs and internal structure of the body. It is possible to consider the ultrasound waves as energy that propagates through a material thanks to the mechanical vibration of its particles. By a direct transfer of energy, the oscillation of a particle around its mean position affects neighbouring particles that start vibrating. The motion direction of the particles can be parallel or perpendicular to the direction of the wave propagation, generating waves that are respectively called longitudinal and transverse waves. The propagation of ultrasound waves differs per material and different physical state, and similarly the wave front geometry. The basic types of waves studied are planar wave, in which the wave front is located on a plane that propagates in space, and circular wave that propagates symmetrically around a reference point, such as sphere or a ring, or around a reference line as a cylinder. Soft tissues are a complex structure in which the energy propagation can be expressed with different types of wave. In general, the shape changes during the propagation and it is hard to attribute to it the ideal shapes that are mostly studied. However, in medical application where the ratio between the transducer diameter and the wavelength is low, the wave generated can be modelled with the spherical wave characteristics [19]. Thus, it is reasonable to consider valid the Huygens' Principle, that states that any wave source can be considered as an infinite collection of spherical wave sources. Since soft tissue has a high content of water, the most used model of ultrasound propagation is simplified with the math of wave propagation in liquids [15]. Considering the motion, along the propagation axis in a certain time, of a particle in an ideal incompressible fluid, the general equation of the propagation is given by [16]:

$$\nabla^2 \phi(x, y, z, t) - \frac{1}{c^2} \frac{d^2}{dt^2} \phi(x, y, z, t) = 0 \quad (1.15)$$

where ϕ is a scalar potential function that models the relation between the pressure and the normalized density change in the media in which the waves propagate, thanks to the compressibility constant K . Instead, c is the longitudinal-wave propagation velocity, that also represents a correction term for sound absorption, whose is modelled to be proportional to the rate of change of the normalized mass density [16]. For a monochromatic wave, the wave propagation can be expressed with the equivalent Helmholtz equation:

$$\nabla^2 \phi(r) - k^2 \phi(r) = 0 \quad (1.16)$$

where:

$$k = \frac{2\pi}{\lambda}, \lambda = \frac{c}{f} \quad (1.17)$$

λ is the wavelength of the ultrasound that is correlated with the frequency and the longitudinal wave velocity. This equation can be solved with different Green's functions [17], considering different boundary conditions. When two waves collide, they exhibit the interference phenomenon: they can form a constructive interference and sum their amplitude or show destructive interference and attenuate their amplitude. If we consider negligible the nonlinear effects, it is possible to consider valid the superposition principle, that states that within an interference zone the net amplitude is the sum of all the interacting wave amplitudes [19].

It is now clear that the wave equation can be simplified with some assumptions and be considered strongly correlated with the density of the material. Studying the behaviour of the wave in different materials permits to characterize and show differences in tissue with a multiple composition. In fact, the main principle of ultrasound imaging is to visualize in an image different materials thanks to the specific ultrasound propagation characteristics. Thus, it is possible to differentiate dissimilar media and, in the medical field, to discover abnormalities in the tissue. To form an US image, sound waves need to be produced, received and interpreted. These operations are accomplished by an ultrasound transducer. There are several transducers that differ each other for differences in centre frequencies, physical dimensions, contact area and shapes. The main characteristic is that the soundwave is produced by a certain number of piezoelectric elements; if a voltage is applied on the two sides of a piezoelectric crystal, it oscillates with a frequency that depends on the crystal thickness. Similarly, when the element is externally excited, a potential is generated. Ultrasound transducers typically consist of 120-512 insulated piezoelectric elements arranged in a linear or curvilinear array. In order to change the dimension of the ultrasound beam window, the array is equipped with a structure that permits to steer the beam in different way. Ultrasound waves are generated in pulses that commonly consist of two or three sound cycle of the same frequency. These pulses must be spaced with enough time to permit the sound to reach the target and return to the transducer before the generation of the next pulse. The Pulse Repetition Frequency (PRF) is the rate of pulses emitted by the transducer and for the medical application, it has a range of 1-10 kHz.

1.2.1 Ultrasound interaction with matter

Characteristic acoustic impedance

To simplify the problem of characterization of different material using the information gathered by the ultrasound propagation it is possible to model the wave as ray and use the laws and assumptions followed by the geometrical optic. The concept of ray is a useful approximation of the path along with the soundwaves propagates under certain circumstances. First of all, the ray propagates in a straight-line

path in a homogeneous medium and it can be absorbed or reflected by the material itself. Different materials respond differently by the passage of ultrasound, depending on the extent to which their medium particles resist to changes due to mechanical disturbance. This property is called characteristic acoustic impedance (Z) and increases in proportion to the density of the material and the velocity of ultrasound in that particular material. The characteristic acoustic impedance, considering a planar wave, may be defined as the product of density and the speed of sound in that material:

$$Z = \rho c \quad (1.18)$$

The table below shows the typical acoustic properties of some tissue [19]; it is important to underline that in most cases the speed of sound varies with temperature.

Tissue or Material	Density ρ [g/cm ³]	Speed of Sound [m/sec]	Acoustic Impedance [Kg/sec m ²] x10 ⁶
Water	1	1480	1.48
Blood	1.055	1575	1.66
Fat	0.95	1450	1.38
Liver	1.06	1590	1.69
Kidney	1.05	1570	1.65
Brain	1.03	1550	1.60
Heart	1.045	1570	1.64
Muscle (along the fiber)	1.065	1575	1.68
Muscle (across the fiber)	1.065	1590	1.69
Skin	1.15	1730	1.99
Bone axial (longitudinal wave)	1.9	4080	7.75
Bone axial (shear waves)	1.9	2800	5.32

Table 1- Acoustic Impedance of some material

When a wave passes from one material to another, or when it encounters discontinuities in the same media, part of its energy is reflected, and part is transmitted with or without changing the direction. In ultrasound application, the wave reflected along a straight line to the source is called echo, while the one that is reflected to other direction are referred as “backscatter”. The portion of material in which the materials show different value of acoustic impedance is called acoustic boundaries, or tissue interfaces. The surfaces hit by the ultrasound wave can be irregular in shape and cause two different type of reflection: specular reflection and non-specular reflection. The first one happens when the ultrasound wave encounters an interface whose boundaries are smooth and larger than the US wavelength, while the non-specular reflection occurs when the dimension of the target is smaller. In this kind of reflection, the particles do not reflect but they vibrate producing spherical wave in all the directions with an

intensity equal to a fraction of the incident beam. In medical image, this phenomenon is responsible of noise and speckle in the US image.

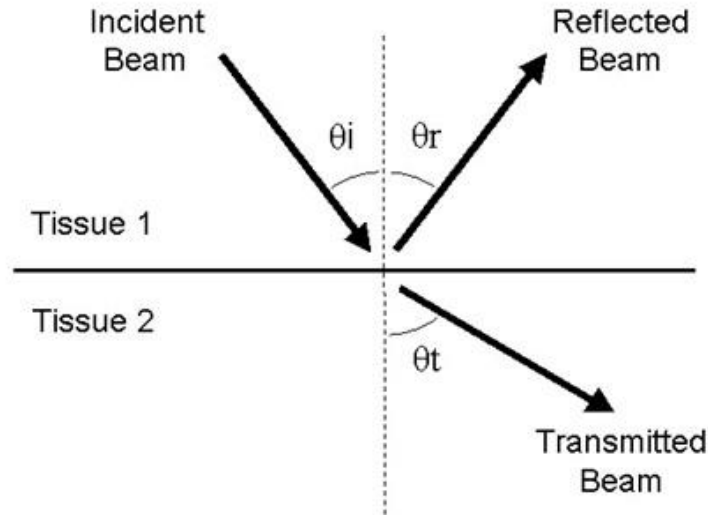


Figure 1. 1 Ultrasound beam [<http://www.usra.ca>]

The specular reflection follows a law similar to that governing the reflection of light; in particular the angle of reflection (θ_r) is the same of the angle of incidence (θ_i), namely the angle between the incident beam and the normal direction to the reflecting surface. Thus, the probability that an echo is detected by the generating transducer, increase as the angle of incidence decreases [15]. Experimental observations have shown that the transmitted wave is deflected according to the transmission angle (θ_t). The value of this deflection is easily demonstrated in optic and obeys the Snell's law, which is defined as [19]:

$$\frac{c_1}{\sin(\theta_i)} = \frac{c_2}{\sin(\theta_t)} \quad (1.19)$$

Where c_1 is the wave speed in the tissue 1 and c_2 in the tissue 2, that are correlated with the acoustic impedance. For this reason, it is possible to correlate the intensity of an echo due to specular reflection with the difference in acoustic impedance values of the two media forming the boundary. The ratio between the intensity of reflected echo (I_r) and the intensity of the incident beam (I_i) can be expressed as [19]:

$$\frac{I_r}{I_i} = \frac{Z_2 \cos(\theta_i) - Z_1 \cos(\theta_t)}{Z_2 \cos(\theta_i) + Z_1 \cos(\theta_t)} \quad (1.20)$$

Where Z represents the acoustic impedance of the materials that form the boundary. This ratio is called reflection coefficient and it represents the proportion of the beam intensity that is reflected from the interface; materials with different acoustic impedance show different intensity of the reflected beam that can be detected by the electronic system and used to differentiate material that compose a specific medium. However, the values of Z for soft tissues are quite similar each other, thus attention should be

focused not on the absolute value of Z , but rather on the comparison of the values in different materials. Considering the energy reflection for normal incidence, it is possible to gather the values showed in the table below [20].

Boundary	% Reflection
Muscle/fat	1
Kidney/fat	0.6
Bone/Muscle	41
Bone/fat	49
Soft Tissue /air	99.9
Soft Tissue/water	0.2

Table 2 Energy ultrasound reflection in some human boundaries

Ultrasound Attenuation

Experimental observations have showed that the amplitude of a planar acoustic waves propagating in a homogeneous medium decrease with the wave travelling distance. This energy loss depends on reflection, scattering, refraction and absorption. The latter refers to the process by which the energy is transformed into a different form of energy, mostly heat. The extent of absorption in media is mainly affected by three factors: viscosity, relaxation time of the medium and beam frequency [20]. In particular, absorption increases with viscosity. The relaxation time is a measure of time taken by particles to revert to their mean positions after a solicitation. When the relaxation time is long, the vibrating particles do not return to their original position before the next disturbing pulse, resulting in dissipation energy due to collision of waves moving in opposite direction. Thus, a long relaxation time of medium causes a high value of absorption. In line of what just described, the absorption of ultrasound increases with the increasing beam frequency because the particles do not have time to revert to their original position if the frequency of the pulses is too high. The reduction of amplitude versus distance of a planar acoustic wave is called ultrasound attenuation, and in nature is exponential. Thus, can be described as:

$$P(x) = P_0 e^{-\alpha x} \quad (1.21)$$

where P_0 is the wave pressure at some reference point, and α is the attenuation coefficient characteristic of each material. Respect to the intensity, the formula can be written as:

$$I(x) = I_0 e^{-2\alpha x} \quad (1.22)$$

The attenuation coefficient depends also on the frequency of the wave. In medical imaging, the attenuation of a specific medium may be quantified in terms of ultrasonic half value thickness (HVT), that correspond to the distance in that medium in which the intensity of the beam reduces to one half its

original value. The table below illustrates the value of ultrasonic HVT in different materials with a frequency of the beam of 2 MHz and 5 MHz [20]:

Material	HVT	
	2 MHz	5 MHz
Muscle	0.75	0.3
Blood	8.5	3.0
Brain	2.0	1.0
Liver	1.5	0.5
Soft tissue (average)	2.1	0.86
Water	340	54
Bone	0.1	0.04
Air (NTP)	0.06	0.01

Table 3 Ultrasonic half value thickness

Table 3 shows that the HVT value for water, and similarly for other liquid, is higher than the other materials. This means that the ultrasound waves can travel long distance in liquids without attenuate their intensity. The main reason of this phenomena is that liquids are acoustically homogeneous and there are no acoustic boundaries within them.

1.2.2 Ultrasound image formation

As described above, ultrasound waves are produced by a piezoelectrical transducer. When a wave encounters an acoustic boundary, some of the ultrasound energy is reflected and interacts with the original piezoelectric crystal. It, converting the energy in electric potential, generates a signal that is electronically processed and measured in order to detect the location of the boundary within the tissue. The set of signals produced along one beam path is referred as a scan line. The ultrasound image is built by collecting a number of scan lines equal to the number of transducers that make up the ultrasound probe. The signals generated by the returning echoes are firstly amplified to increase their intensity. Moreover, in order to reduce the effect of acoustic attenuation in the media, they are subjected to a time gain compensation (TGC). This process applies different amplification to signal received from different tissue depth: echoes originating from longer distance are more amplified that those from short distances. There are many ways to visualize the signal and it depends on the characteristic of the probe, the scope and the physical properties of the tissue to be imaged.

The simplest way of visualization is **A-Mode**, Amplitude Mode. It consists of displaying the amplitude of 1D echoes of a single pulse, as a function of the distance it has traveled in the direction of propagation. The signal echoes are transformed in the form of spikes by a cathode ray oscilloscope (CRO). Thus, the

position of a spike in time is associated to a measure of distance between the position of the reflecting boundary and the transducer.

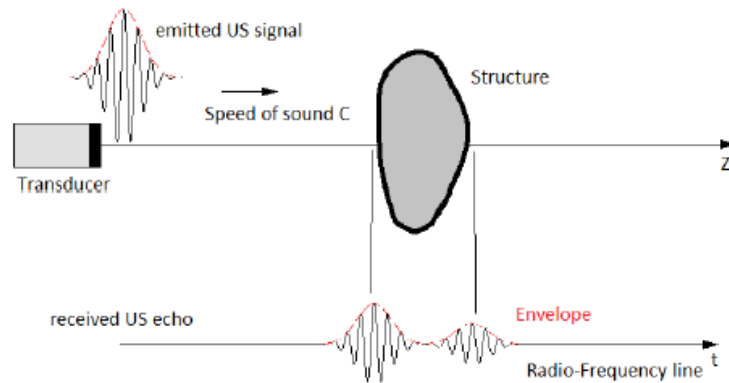


Figure 1. 2 A- Mode visualization [18]

The **B-Mode**, brightness mode, is the display of 2D map composed by dots of varying intensities, corresponding to the echo intensity evaluated with the same modality of the A-Mode. The z-axis of the image correspond to the distance of the boundaries and the brightness of each dots is correlated with the intensity of the echo generated in that specific position. The B-mode is used for real-time imaging: numerous images are generated repetitively at a rate exceeding about 25 frames per second to create the impression of continuity in time. This modality is the most used in medical application, and in particular for assisted breast biopsy because allows the simultaneously visualization of the lesion and the needle insertion. Other visualization modalities are **M-Mode**, a time motion display of a chosen ultrasound line, and the **Doppler mode** that make use of the Doppler effect to measure and visualize fluids flow.

1.2.3 Ultrasound resolution

Spatial resolution

Spatial resolution represents the ability of the Ultrasound system to distinguish two structures close to each other. It depends on the contribute of the medium and at the same time on the frequency characteristic of the ultrasound transducer.

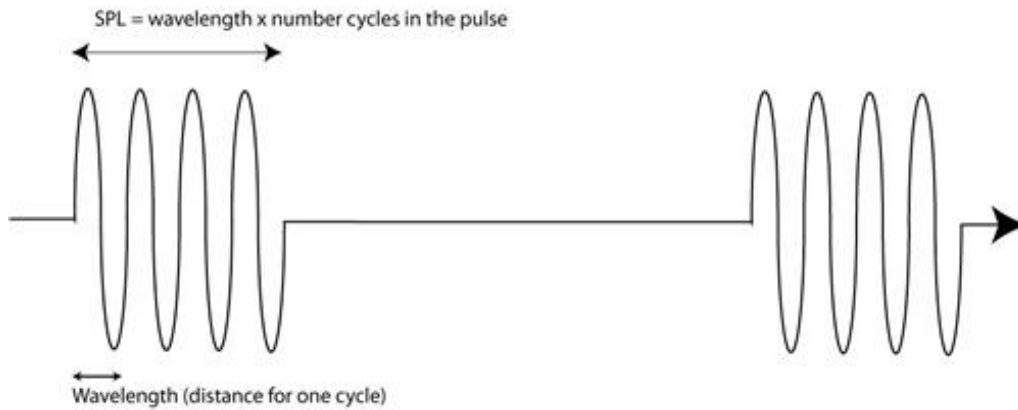


Figure 1. 3 Series of ultrasound pulses <https://sites.google.com/site/ektasphysicseportfolio/spatial-pulse-length>

It is defined as the product of the number of cycles in a pulse of ultrasound and the wavelength:

$$SPL = \#cycles\ in\ pulse \times wavelength\ (mm) \quad (1.23)$$

Most pulses consist of two or three cycles, the number of which is determined by the damping rate of the piezoelectric elements of the ultrasound transducer [24].

Axial resolution, also called longitudinal resolution, is the minimum distance that can be differentiated between two elements located parallel to the direction of the ultrasound beam. Mathematically, it is equal to half the spatial pulse length.

$$Longitudinal\ Resolution = \frac{SPL}{2} \quad (1.24)$$

For the piezoelectric nature of the transducer, the wavelength of the ultrasound beam is equal to twice the thickness of the element in the transducer. Having a good longitudinal resolution means that the damping rate of the ultrasound transducer is high. However, an excessive damping is associated with loss of amplitude and hence to a low-intensity ultrasound beam. Moreover, soft tissue attenuates high-frequency pulses, which means that wave with high frequency are not able to be reflected back with a detectable intensity by deep boundaries [24].

Lateral resolution is the minimum distance that can be distinguished between two targets located perpendicular to the direction of ultrasound beam. It is strictly correlated with the beam width that varies with the distance of the transducer. The beam width at the beginning is approximately equal to the width of the transducer, then converges to its narrowest width, equal to half of the width of the transducer, at a distance called the near-zone length. At a distance greater than this zone, the beam diverges such it

becomes the width of the transducer at a distance twice than the near-zone length [24]. So, lateral resolution is determined by the equation:

$$\text{Near zone length} = \frac{\text{Area of transducer}^2}{4 * \text{wavelength}} \quad (1.25)$$

Thus, it can be implemented using focusing techniques, that create focal region within the near zone, reducing the near-zone length to a shorter value called focal length. It permits to have an optimal resolution in the region of interest and to increment the lateral resolution in that zone.

Contrast resolution

Contrast resolution refers to the ability to distinguish between different echo amplitudes of adjacent structures. It may be enhanced at various stages in the image processing, including compression of the dynamic range, image memory and use of contrast agents. The ultrasound image is made by pixels. The visualization of various shades of grey depends on the number of bits of each pixel, that has to be the highest possible. For example, a 5-bit memory enables 32 shades of gray to be stored [24], and thus to have a higher contrast resolution and a better quality of the image.

1.2.4 Artifacts of ultrasound image

Ultrasound artefacts can be grouped in different ways depending on the ultrasound modality, such as B-Mode or Dobbler mode, but also on the type of assumptions that they violate, such those related to the internal structure of the ultrasound transducer, or those that are primarily related to beam properties and processing. In short, the principal assumptions used in ultrasound evaluation are that pulses and echoes travel along a straight path, echoes return to the transducer after a single reflection and travel at a uniform speed of 1540 m/s and that the attenuation is uniform by all the tissues [27].

The **reverberation artifact** violates the assumption that an echo returns to the transducer after one reflection, and it is usually caused by significant differences in the acoustic impedance of two adjacent tissues [26]. A portion of a reflected echoes encounters another reflector and it reflect a second time before going back to the transducer. This is interpreted by the system as a boundary that is further away than the original structure. The **comet tail artifact** is caused by multiple reverberation from multiple closely refractors.

Similarly, in the **mirror image artifacts** the ultrasound wave is initially reflected from the original object and then encounters a highly reflective structure that reflects again the wave that hits for a second time the initial object with a different incident angle. This phenomenon causes two different echoes of the same object that is displayed twice equidistant and on the opposite side of the reflector, creating a mirror image. Luckily these artefacts are usually easy to detect because they are very recognizable.

Acoustic shadowing violates the assumption that echoes are attenuated equally by all the tissues. Indeed, this artefact is caused by a partial or complete attenuation of the ultrasound beam along its path in a specific media, which is responsible of a loss of signal and a consequent shadowing of the image. A very common problem is the shadowing caused by air that forms an impenetrable barrier to sound causing a very poor-quality image. The **enhancement artifact** is caused by a material that has an attenuation coefficient higher than the one assumed and produces a too bright image with a consequently reduction of the quality.

The **speckle artifact** is determined by the interference of objects that are too small to be detected by the ultrasound beam. The resulting image appears noisy and characterized by a granular texture. Modification of spatial resolution and frequency may help to reduce this artifact.

Refraction artifact follows the physical law of refraction that assumes that when a beam encounters a tissue interface it changes its direction according to the tissue refractive index. This entails that objects that are not truly in the scanned field of view can be artifactually represented on display, causing object position misregistration, duplication or lateral defocusing of curved edge [26]. These artifacts are easily recognizable because show in the image anatomically impossible structure and can be eliminated by changing the angle and the position of the transducer.

Beam width artifact violates the assumption that echoes are generated only by one reflector. It occurs when an object is located after the beam focal zone and creates false detectable echoes that are displayed as overlapping the structure of interest.

The **range ambiguity** artifact is since an error of pulse assignation can be made when pulses of high frequency are used. In particular, the information related to the echo of one pulse can be wrongly associated to the following or previous pulse. In order to reduce this artifacts, it is possible to reduce the pulse repetition frequency.

The **speed error artifact** occurs when the assumption of the fixed velocity of sound in tissue is violated. For example, ultrasound wave travels fatty tissue with a velocity lower than 1540 m/s and in this media shallow objects may be misrepresented in the image as deeper.

To reduce the effect of these artifacts is possible to change the orientation of the US probe, the pulse frequency of the transducer or to use post-processing image techniques in order to improve the image quality and clarity.

1.2.5 Acoustical properties of some polymers

One of the peculiar properties that the pressure sensor to design must have is the acoustically transparency. It means that the ultrasound wave does not have to be attenuated by the material itself, and

the intensity of the reflected wave at their boundaries must be as lower as possible in order to have a high-intensity wave in the soft tissue to analyze. The pressure sensor is in contact with the human skin; having a low-intensity reflected wave means to have a material with an acoustically impedance close to the acoustic impedance of the skin. In literature there are several studies in which the optoacoustic properties of different materials have been studying to develop phantoms able to mimic soft tissue optical and acoustic properties. The development of these phantoms is an important tool for testing and optimization of medical ultrasound system for medical training [30]. Studies have shown that materials that mimic efficiently soft tissue are hydrogels, a group of polymeric material with a hydrophilic functional group attached that is able to absorb a great amount of water. Because they are mainly consisting of water, they have low acoustic attenuation and an impedance coefficient and a speed of sound similar to biological tissue. The most common hydrogel materials are polyvinyl alcohol gel (PVA), polyacrylamide gel (PAA), gelatin and agar [30]. They show very good acoustic properties and an acceptable stability over time. Another very common material is Polyvinyl Chloride-Plastisol (PVCP), a white opaque solution of monomers that polymerizes in a non-toxic plastic and it's insoluble in water. Plastisol changes its structure when heated around 200°C becoming transparent. It is usually mixed with other particles to acquire better mechanical properties or to obtain specific optic properties that better mimic the behavior of soft tissues [28,29]. This material is very easy to manufacture in several different geometry with an acceptable structure rigidity; it shows chemical and elastic stability and for these reasons it is used for tissue mimicking. Cafarelli et al. [30] have studied the acoustical properties of polydimethylsiloxane (PDMS), a silicon-based organic polymer widely used in microelectromechanical systems. It shows an acoustic impedance value slightly higher than PAA, and an attenuation coefficient significantly higher. However, the latter value increase with the material concentration and quantity of material exposed to sound wave. Thus, the effect of interposing a soft sensor constituted of PDMS between the skin and the ultrasound transducer is unknow, and it is hard to suppose this effect using the only knowledges of the acoustic properties of the materials that compose it.

2. TACTILE PRESSURE SENSOR

Women breast is characterized by several type of tissues; in particular they are made up lobules and ducts necessary to the production and transportation of milk, covered by fibrous and fat tissues that give the breast size and shape. The composition can change during lifetime and is peculiar for each woman. Tissues differentiation capability is one of the main goals to aim in the design of the pressure sensor. Commercially medical devices able to asses elastographic data are described in the chapter 1.1. One example is the SureTouch system that exploits the mechanical elastography method.



Figure 2. 1 SureTouch [37]

It is an FDA-cleared medical device that provides a painless breast exam with the use of an array of tactile sensor mounted on a handheld probe. As the probe is pressed against the breast, the sensor array captures varying reaction pressures caused by differences in tissue hardness. The probe head measures 50 x 40 mm with a curvature radius of 38 mm, and it is made of 192 pressure sensors arranged in an array (16 x 12) that covers a surface of 40 x 30 mm [37]. Each pressure sensor has a rectangular pressure sensing area of 2.5 x 2.5 mm with a sensitivity of about 0.05 kPa [12]. SureTouch provides a 3D image of the breast with a quantitative evaluation of relevant lesion features, such as size, shape, hardness, heterogeneity, and mobility. Therefore, mechanical elastography, simulating manual palpation, aims to reconstruct the composition of a volume of tissue from surface mechanical measurements. The same problem is debated and studied in Robotics, where it is necessary to have a system able to create a map

of the environment in which the robot has to operate. While optical vision can recognize the surface of a material, the sense of touch is able to identify material texture and composition. This property replicates exactly the human sense of touch and it is usually made by a tactile sensing system, that consist of flexible touch sensing arrays, access electronics and algorithms for data sampling and processing. It plays a fundamental role in the manipulator control system since it can estimates contact parameters between the robot and the environment such as contact force, slip, hardness and texture. These functions are important constituent for the manipulator safe interactions and permit to resolve object recognition and grasping problems and to characterize different materials by their mechanical properties. Soft tactile sensors are realized via a variety of electronic structures and materials; the most common are made by piezoresistive composite or liquid metal conductors embedded in a polymer material, such as PDMS or other photocurable rubbers.

The main idea is to use a capacitive tactile sensor that is able to mimic the SureTouch ability of tissue differentiation and to implement the control loop of the robot. Mechanical imaging techniques based on soft sensor could facilitate imaging of sensitive, curved, hard or heterogeneous tissues and could capture quantitative data during existing clinical physical examination practices [14]. According with the current method used for mechanical elastography, an array of soft capacitive tactile sensors can provide the same tissue mechanical information gathered by the SureTouch medical device. In this chapter, some characteristics of two soft capacitive tactile sensors are evaluated and compared with the performance of SureTouch. However, there is no studies that estimate the interaction of ultrasound waves with the components of tactile sensor; thus, the primary constrain of acoustically transparency cannot be evaluated and it is not possible to consider the usage of tactile sensors as a real solution for the MURAB project.

2.1 Capacitive soft sensors

The sensing modality of the capacitive tactile sensors considered in this evaluation, uses variation of electric charge between two stimulated plates to describe the pressure distribution above their surfaces. For a parallel plate configuration, the easiest expression of capacitance is:

$$C = \frac{\epsilon_0 \epsilon_r A}{d} \quad (2.1)$$

where A is the overlapping area of the plates, d is the distance between the plates and ϵ_0 and ϵ_r represent respectively the permittivity of vacuum and the dielectric constant of the material between the two plates. While the numerator of the expression is fixed by the geometrical constrains of the sensor, the variation of the d value results in a change of capacitance. If the plates are connected to an electrical

circuit, the capacitance can be expressed as the ratio of the charges on the plates (q), and the voltage between the plates (V).

$$C = \frac{q}{V} \quad (2.2)$$

This value can be detected by an electronic circuit and it is strictly correlated with the distance variation of the two plates. Thus, the application of forces to the sensor plates cause a different relative position of plates and consequently a capacitance variation that is detected by the electronic circuit.

The capacitive soft sensors considered are made of two layers of conductive channels in a substrate of a stretchable polymer. The one proposed by Shanshan [39], is made of highly conductive silver nanowires (AgNW) patterned by screen printing in a Silica substrate and transferred to a PDMS layer. Two layers of PMDS – AgNW composite are positioned orthogonally and laminated together with an Ecoflex film. Instead, Bin Li et al [38] propose a sensor made of two groups of microchannels filled with eGaIn and embedded on separate planes with orthogonal orientation in a silicone polymer substrate. A picture of this sensor is represented in the Figure 2.2.

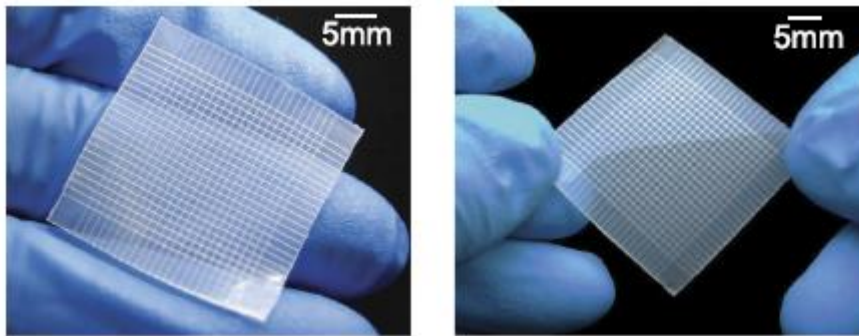


Figure 2.2 Capacitive Tactile sensing [38]

As the structure of these two sensors is more complex of the case of two conductive plates, the expression of the capacitance expressed before cannot be used. However, it is possible to define a model for electrical capacitance between a pair of orthogonally conductive microchannel, by combining the electrostatic method of images, the superposition principle, and elements of transmission line coupling theory [38]. The models used in both sensors are described in the relative papers.

2.2 Sensor Performance

Sensor performance describes several instrumentation testing, diagnostic and analysis techniques to verify the reliability, health and performance of a sensor process. Static accuracy describes how closely the sensor signal represent the actual measured being monitored, after the transient period. The static calibration curve, also known as transfer function, plots the output amplitude vs different inputs and visually shows some characteristic of the sensor as:

- **Sensitivity** is a measure of output change relative to a unit change in the input. It represents the slope of the transfer function.
- **Resolution** is the minimum detectable input signal.
- **Range** is the sensible range of input and output of the sensor.
- **Linearity** describes how well a straight line approximates the calibration curve over the specific range. The nonlinearity error corresponds to the maximum deviation of the actual measured value from a linear transfer function.
- **Drift** is the deviation from a specific reading of the sensor when the sensor is kept at that value for a prolonged period.
- **Precision** is the capacity of a measuring instrument to give the same reading when repetitively measuring the same quantities under the same prescribed conditions. This term is closely related to repeatability, that is the precision of a set of measurements taken over a short time interval, and reproducibility that consider a set of measurement taken over a long-time interval and performed by different operator with different instruments and in different laboratories.
- **Over force** is the maximum force which safely may be applied to the sensor.
- **Hysteresis** is the dependence of the system on its history and represents the difference in output when any value of the measurand is approached from the low and the high side.
- **Dynamic characteristics** represent the time response of the sensor system and include rise time, delay time, peak time, setting time. The dynamic linearity is a measure of the sensor ability to follow rapid changes in the input parameters.

Moreover, two other characteristics are important to determinate the sensor quality. One of these is **lifetime**, which represent the effective time in which the sensor remains sensitive and functional under normal operating conditions, and **temperature range** that is the range over which the sensor produces an output proportional only to the force.

In order to verify if the two conductive tactile sensors previously described have the same capability of the SureTouch system, some information about sensor performance are gathered and reported in the table 4.

	Soft tactile sensors		
	SureTouch [12]	eGaIn [39]	AgNW [38]
Pressure distribution	√	√	√
Measurement area	40 x 30 mm	23 x 23 mm	
Sensitivity	0.05 kPa		0.57 MPa
Range		50 – 450 kPa 0 - 240 %	0 – 50 %
Spatial resolution	2.5 x 2.5 mm	1 X 1 mm	2 X 2 mm
Nr. of elements	16 x 12	8 X 8	7 X 7
Hysteresis	2% - 4%	3%	

Table 4 Comparison of some SureTouch and tactile sensors characteristics

It is evident that the soft tactile sensor evaluated are less performing that the capacitive sensors used in the SureTouch medical device. It is demonstrated that the sensitivity of sensors made of carbon nanotube electrodes shows a sensitivity of 0.23 MPa over the pressure range up to 1 MPa, and those with serpentine gold electrodes a sensitivity of 0.48 MPa [38]. However, Bin Li et All [14] have verify that the sensor made of soft polymers and microfluidic electrodes, described in the section above, has the capability to perform mechanical elastographic measurements. The tactile sensor described is integrated to a circuit for capacitance measurement (AD7746, Analog Device) and is able to robustly image lumps in soft tissues [14]. Soft tactile sensors are gathering increasing attention in the scientific world, and a great number of research groups are developing new fabrication machines able to print customizable electronic circuit over a polymer substrate. Thus, there is reasons to believe that the use of soft tactile sensors for elastographic measurements, will be a commercially solution in the next future.

3. ULTRASOUND PRESSURE SENSOR

The idea promoted by the University of Twente is to use a pad of an acoustically transparent material and the ultrasound imaging to detect the pressure on its surface. While the mechanical model and the sensing modality of this type of sensor are described in the first section of this chapter, the second section summaries some considerations about the design of the sensor and some possible implementations.

3.1 Sensing modality

The sensor is a rectangular shape pad made of a controlled percentage of Platisol and plasticizer that contribute to vary the stiffness of the material. It is designed to fit over the US probe, and it is fabricated by a molding process.



Figure 3. 1 Ultrasound pressure sensor concept [40]

The first assumption is to consider the pad made of a material that returns to its original shape when the loads are removed following a linear elastic model. Assuming that the total strain is small, the relation between the strain and the stress is defined by the Young's modulus (E) of the material. For simplicity, the stress applied is considered normal to the material surface with a consistent strain only in one direction. Thus, stress and strain relation can be simplified in this form:

$$\sigma_{zz} = E \cdot \varepsilon_{zz} \quad (3. 1)$$

where σ_{zz} defines the normal stress applied along the z-axis, and the ε_{zz} the strain associated. The strain is a measure of deformation representing the ratio between the displacement (Δl_z) between two point of the material and a reference length that is usually the absolute length (L_z) of the material considered. Mathematically, can be expressed as:

$$\varepsilon_{zz} = \frac{\Delta l_z}{L_z} \quad (3. 2)$$

The displacement of the material after the application of a normal force, can be sensed with different methods and technology and permits to calculate the relative stress and thus the overall force applied to the material.

$$\sigma_{zz} = \frac{F}{A} = \frac{E \cdot \Delta l_z}{L_z} \quad (3.3)$$

The main idea of this type of sensor is that the displacement is measured thanks to the evaluation of ultrasound images. The figure below shows the US image of a phantom made of two different materials (M1, M2). The phantom is pressed by a transducer covered with a 3 mm thick pad sensor. Boundaries between different materials are visible, and it's possible to define three different regions: the upper one represents the pad itself, the middle and the lower part are characterized by the different materials of the phantom.

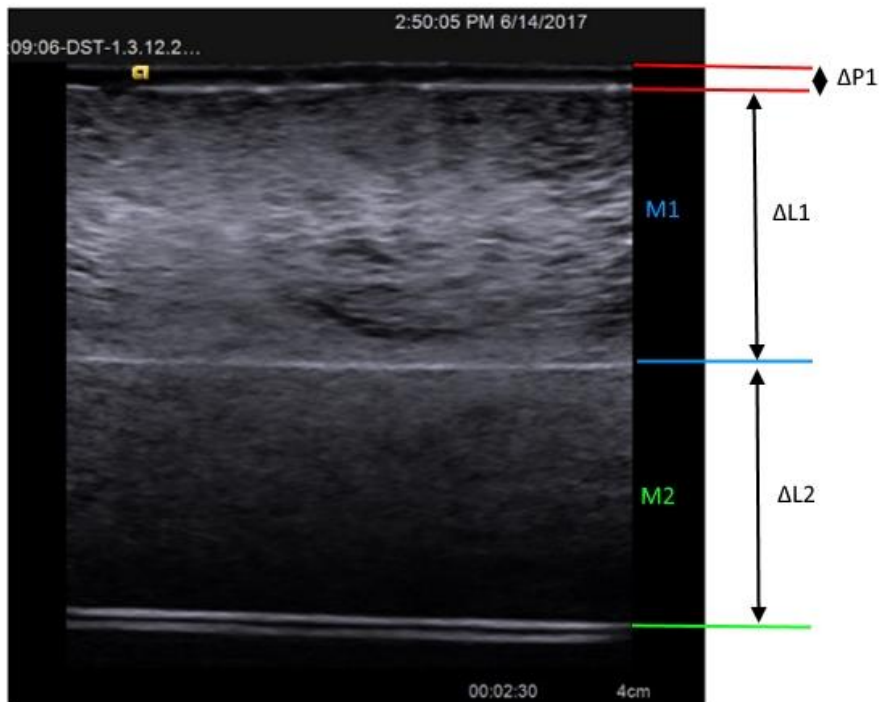


Figure 3.2 Ultrasound image: view of pressure sensor and a phantom made of 2 different material

The sensing modality is defined by measuring the thickness of the material, using the images gathered from the US detection, under unknown pressures. The idea is to have a pad made of a material completely characterized and of which the elastic modulus is known. The value of the displacement, the initial length of the pad and the Young's modulus, permit to obtain the overall stress applied to the phantom. This value can be correlated with the displacement of the other materials and associated with an elastic modulus. The measurements from the US images are processed manually; the thickness of the pad is measured by counting the pixels at different spots on the boundaries and averaging them. The

measurement area of the pad is the same of the active surface of the ultrasound probe used, around 50 mm². Since the ultrasound transducer has to scan the entire surface of a breast without causing pain to the patient, the sensor has to be sensible to small forces, up to a maximum value of 20 N.

3.2 Sensor considerations

According to the works made previously by the RaM group at the University of Twente, the pad has to fit well onto the probe and has to have an area equal to the surface of the transducer. To fulfill this requirement, a complex mold is used, showed in the figure 3.3.



Figure 3. 3 Mold for manufacturing the ultrasound pressure sensor [40]

A model of the ultrasound probe used for the experiment is designed and 3D printed. It is used as a part of the mold, that consists in a lower part with dimensions slightly bigger than the ultrasound probe and an external structure able to hold the 3D printed ultrasound probe and change its position. The Plastisol mixture is poured into the lower part of the mold and solidifies in the specific shape showed in figure 3.1. With this type of mold, it is possible to varying the thickness of pad, and consequently the range of measurements detectable. In particular, considering an application force of 10 N and supposing the pad made of a material with an elastic modulus E equal to 50 KPa, the theoretic strain percentage is:

$$\varepsilon = \frac{F}{A \cdot E} = 4 \% \quad (3.4)$$

This means that if the pad has an initial length of 1 mm, the displacement is equal to 0.04 mm. This value is too much low and the ultrasound image is not able to detect any depth variation. Thus, the ultrasound pressure sensor described, can work only if the initial depth of the sensing area is long enough to show a displacement that can be detected by the ultrasound images that, as described in Chapter 1.2, have a specific resolution and are affected by image artifacts. Therefore, the correct approach for improving this type of sensor is firstly to evaluate which is the minimum pad depth necessary to use the

ultrasound imaging as sensor technology. However, this value is strongly correlated with the composition of the pad and the mechanical elasticity that it exhibits.

So, the approach to follow for the ultrasound pressure implementation can be summarized in:

1. Study the best material composition for the Ultrasound Pressure sensor. It has to be acoustically transparent and strong enough to be fitted in the ultrasound probe.
2. Study the mechanical compression behavior of the new material and evaluate its elastic modulus. To do this evaluation, it is necessary to have a material tester with a simple geometry that can be easily reproduced. An example of tester material is reported in Chapter 4.
3. Once the material is fixed, evaluate tester pads with different depth length, with the ultrasound imaging.
4. Compare the results, such as image quality, sensor linearity and sensor range, to study the pad depth that best fit this problem.
5. Manufacture the ultrasound pressor sensor with the desired shape using the mold of figure 3.3.
6. Test the capability of tissue differentiation.

In this thesis, a tester material is produced and a method for determining the sensor sensitivity is proposed.

4. MATERIALS AND METHODS

This chapter collects the materials and methods used to test the material and the use of the ultrasound pressure sensor described in Chapter 3. First of all, the manufacturing procedure to build up a tester pad of an acoustically transparent material is described. This tester is used in three experiments, made to test the accuracy and feasibility of the ultrasound pressure sensor. To evaluate the displacement of the pad under unknown pressure, it is firstly necessary to find a correlation between the image parameters and the pad length measurements. Thus, a process of calibration is needed in order to find the length resolution of a pixel of the ultrasound image. The resolution of a pixel permits to evaluate the real depth of the pad counting the number of pixels between the pad boundaries showed by the ultrasound image. In the second experiment, the relation between stress and strain is roughly evaluated. In particular, the measures of pad depth under known pressures are gathered. This evaluation estimates a numerical value of the relation between force and deformation, which is necessary to predict the pressure applied knowing the variation in depth. It also represents the sensitivity of the ultrasound pressure sensor. In order to verify the possibility of adding the information of the pad displacement in the system control of the robot, the third experiment verifies the correlation between the pad displacement with the ultrasound probe movement. It is measured thanks to a laser sensor connected with an Arduino board. This chapter describes the experiment set up and the methods used to gather and process data.

4.1 Pad manufacturing

The material chosen to produce the acoustically transparent pad is the LUPA Medium Plastisol. It is a thermoplastic liquid polymer made by a mixture of PVC resin, plasticizer and stabilizer. It has the peculiarity to become transparent with high temperature, thanks to which all the component fuse together to form a flexible vinyl solid that is quite stable and durable. It is flame retardant and resistant to chemical damage and it use in a wide range of applications from medical product development to automotive market.

The tester material is made with a molding process. In order to create the final polymer product, Plastisol has to be heated and then poured into the mold. Thus, the mold has to be made by a temperature resistant material.

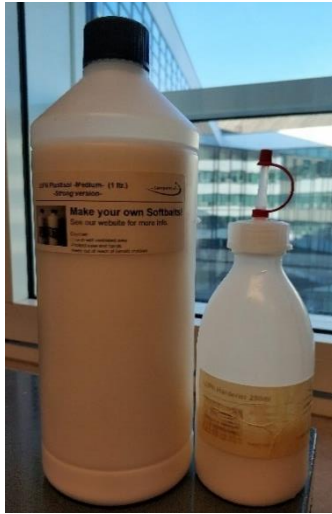


Figure 4. 1 Plastisol and hardener

The geometry of the mold is very simple; it is a 50 x 20 x 30 mm box with a drilled cover that has the purpose to protect the polymer and avoid the contact with the air during its cooling. It is drawn with PTC Creo Parametric and printed with the Ultimaker S5 printer. The material used is White Tough PLA plastic, which is a technical PLA filament less brittle than regular PLA and with a toughness comparable to ABS.



Figure 4. 2 Three views of the mold used

The pad used as tester in the experiments described in the following chapter, has to fulfill the specific characteristic of acoustic transparency. The ultrasound waves should pass through the material without any interference and be reflected by the surface under the pad. Traducing this phenomenon in imaging means that the ultrasound image has to show a bright line, corresponding to the reflection of the surface, that can be automatically recognize and evaluated in order to quantify the depth of the pad for detecting

the pressure applied to it. The acoustically transparency is due to the composition of the material and its homogeneity. The presence of air bubbles inside the material causes scattering and dispersion of sound wave energy; the image produced by the ultrasound system is totally black and does not contain any useful information. The figure 3.5 shows the second pad produced. It is made by 82% in mass of Plastisol, 14% of hardener and 4% of Silica gel, a cheap powder used to produce phantom which better mimic the skin behaviour. The pad is solid with a rigid structure; however, it is possible to notice visually the presence of air bubbles inside. As the Ultrasound image shows, the scattering is too high to permit a correct visualization of the inferior boundary of the pad. Thus, the material is not acoustically transparent, and the tester could not be used in the experiment.

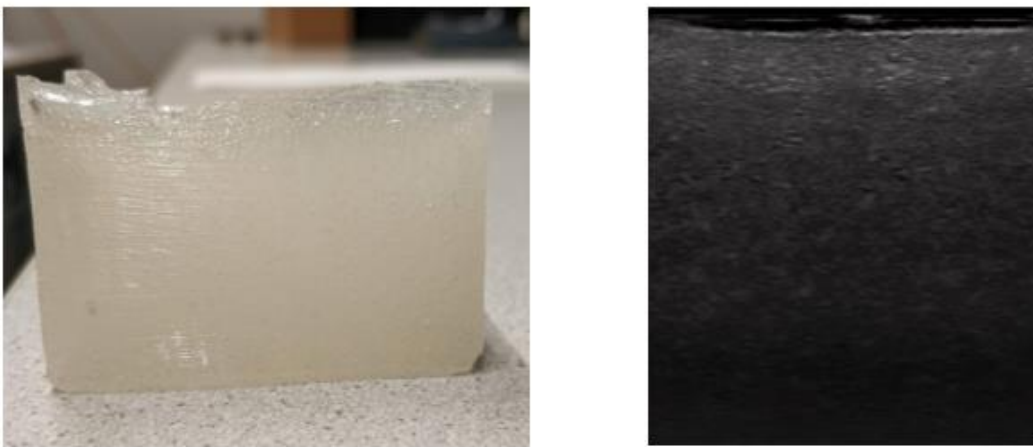


Figure 4. 3 II pad with its ultrasound image. The pad is not acoustically transparent

In order to remove the air bubbles inside the material, it is used a vacuum oven with a compressor. In particular the procedure utilized for the correct pad is described below:

- 1) Mix 92% in mass of Plastisol medium with 6% of hardener and 2% of Silica gel in a pan
- 2) Put the pan on a heating plate on 200° Celsius with a magnetic stirrer set to 180 rpm



Figure 4. 4 Heating plate with a magnetic stirrer

- 3) Wait until the mixture becomes transparent
- 4) Put the pan into the vacuum oven (Heraus VT 5042 EK) with a temperature of 200°C and a pressure of 200 bar for 20 minutes
- 5) Put the pan on the heating plate with the magnetic stirrer for 10 minutes and cover it with a lid
- 6) Pour the mix into the mold and cover it
- 7) Let it cool down until solid
- 8) Remove the pad from the mold

The result is showed in the figure 3.7. The ultrasound image is characterized by a bright white line that represent the surface under the pad.

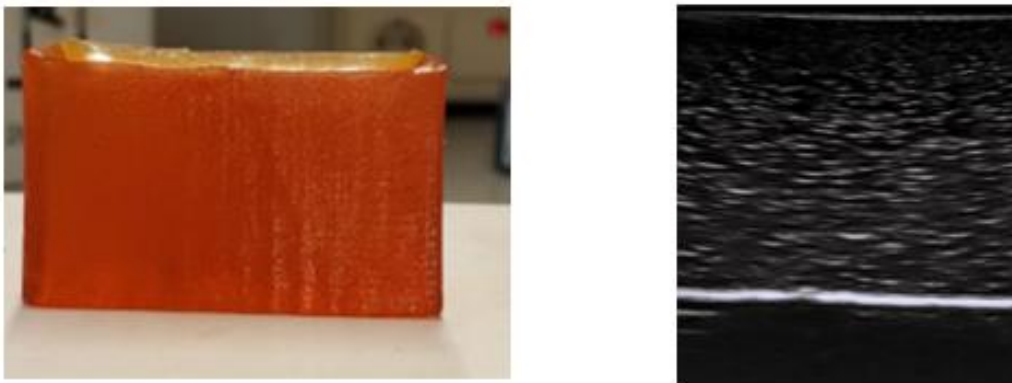


Figure 4. 5 IV pad with its ultrasound image. The pad is acoustically transparent

The pad is rectangular shape and its dimensions are 47.2 x 18.8 x 23.4 mm. The color is orange, probably due to the long exposition of the mixture to high temperature. However, the ultrasound image clearly shows the line of the reflected surface under the pad, thus the tester is acoustically transparent. The image appears noisy and with a stippled texture; visually it is possible to notice that the pad has bubbles and presents impurities and inhomogeneities that are shown by the ultrasound as random lines. In addition, there are white lines under the brightest boundary, and these probably are due to some ultrasound artifacts, such as the reverberation one. In order to reduce these effects, the image can be processed using several algorithms, filters and image segmentation.

4.2 External set-up

The ultrasound system used for the experiment is the Acuson P500™, a portable system produced by Siemens Healthcare. It is implemented with the L10-5v linear transducer composed by 128 piezoelectric elements with a frequency bandwidth of 5-12 MHz and a footprint of 38.4 mm [31]. For its ergonomic

design and the user-selectable frequency, this type of linear transducer is highly indicated for breast evaluation.



Figure 4. 6 Ultrasound system [31]

To acquire the ultrasound image a Magewell USB Capture HDMI device is used. It permits to connect the HDMI port of the ultrasound system with the USB port of the laptop. The device can handle video resolution up to 2048 x 2160 and a frame rate of 120 fps, which is sufficient for this application. The images captured represent the screen displays by the ultrasound system. Thus, images need to be cropped.



Figure 4. 7 Magewell USB Capture HDMI [32]

The idea of the experiment is to force the movement of the ultrasound probe only in the vertical direction, normal to the pad surface. For this purpose, the ultrasound probe is fixed to a slider with some components that are 3D printed for this application. The slider is then fixed to a steel base structure. The figure below shows the final structure and the parts designed.

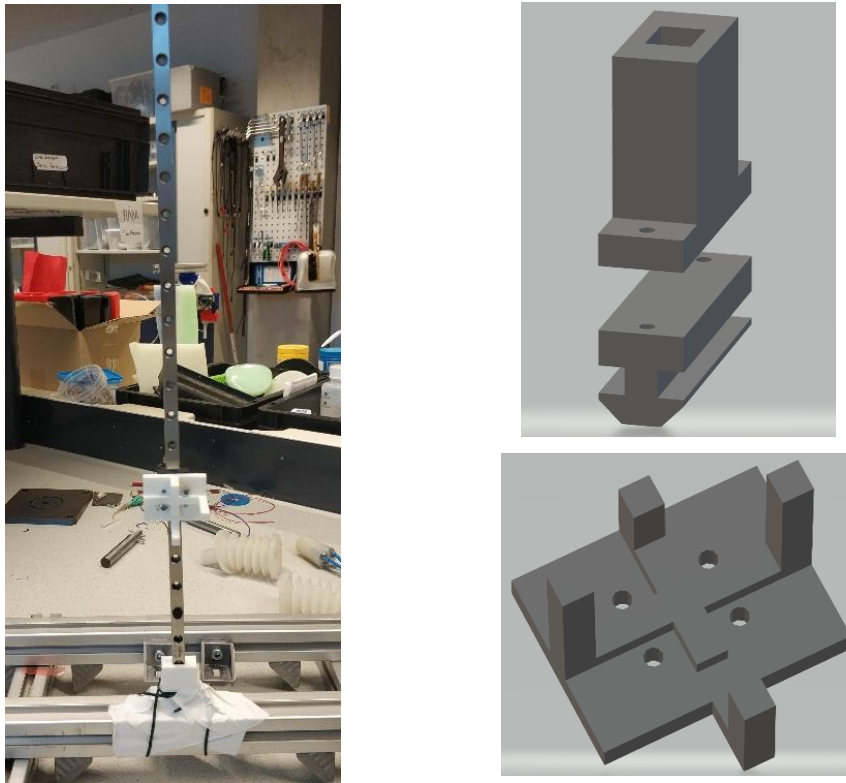


Figure 4. 8 External set up

4.3 US images post-processing

The ultrasound images are captured by the Magewell USB Capture HDMI device thanks to a Matlab script. In order to have a more precise estimation of the data processed, ten sequentially images are captured by the system, cropped and saved in a specific folder. The main code used to accomplish this operation is reported below.

```
%create a new folder with a specific name
destinationFolder = 'D:\Twente\Experiments'
folder = '2nd_PAD';
mkdir(folder)
cd(folder)

for i=1:10

    img = snapshot(cam);
    img_crop = imcrop(img,[684 57 436 580]);
    name = 'Pad2';
    out = sprintf('%s_%d.%s',name,i,'jpg');
    imwrite (img_crop, out);

end
```


The image is cropped so as to have the first line of the new image correspondent to the first line of the ultrasound image, that is the contact point of the ultrasound probe with the pad. The image 4.4 shows the resulting cropping made by this code. The image is then post-processed in order to evaluate the number of pixels between the upper line and the brightest line.

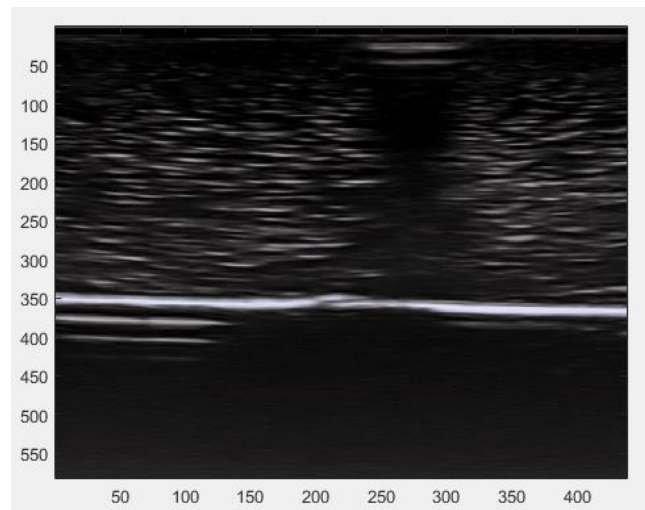


Figure 4. 9 Cropping image Matlab script result

As it possible to notice the ultrasound image is noisy and characterized by random lines. In order to improve image quality and minimize the effect of these errors, the image is processed with a method for estimating a per-pixel confidence in the intensity of the US image. It is referred as confidence map, and

it is defined as the probability that an echo, originating from a specific pixel, reaches one of the transducer elements [33]. This algorithm transforms the image in a black and white image in which each pixel has a value between 0 and 1. It is controlled by three different values: the α parameter considers the effect of acoustic attenuation and scaled the confidence in the vertical direction. The parameter β is related to acoustic absorption and change the effective contrast in the confidence map and the γ parameters penalizes horizontal and diagonal random walks [34]. The optimal parameter settings are dependent on the internal structure of the material to evaluate, and for this application the α , β and γ parameters are setting respectively as 4.0, 120 and 0.09. The effect in using this algorithm is showed in the image below.

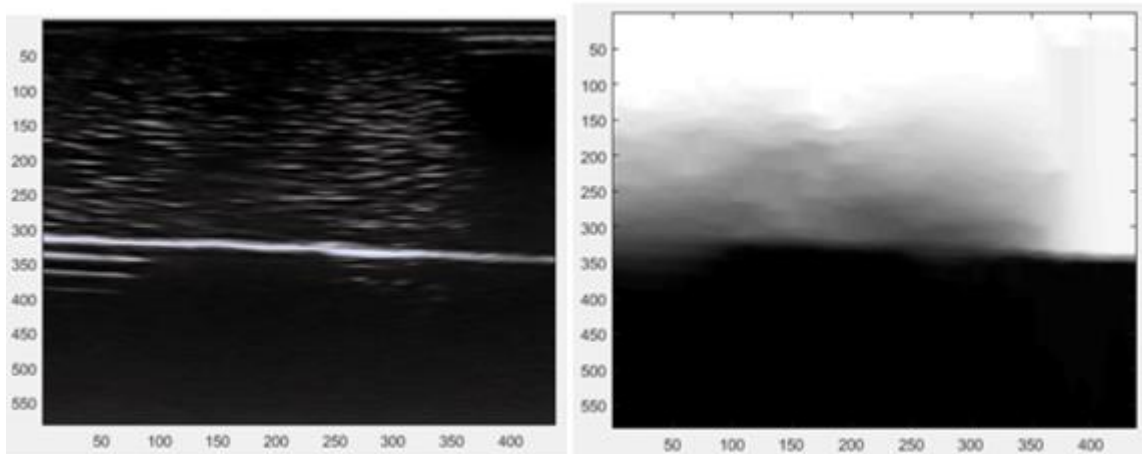


Figure 4.10 Confidence map

Then it is easily possible to write a code able to recognize the position of the boundary between the bright and dark portions of material. In particular for each column it is find the position of the pixel with a numerical value lower than the threshold value, set to 0.3. All these values are then averaged in order to find a single value for the image. The final pad depth measurement is the mean of the values obtained from the 10 images evaluated.

```
for i=1:10

    out = sprintf('%s_%d.%s',name,i,'jpg');
    img_crop = importdata(out);
    img = rgb2gray(img_crop);

    %%Confidence map
    alpha = 4.0; beta =120; gamma = 0.09;

    [ map ] = confMap(img, alpha, beta, gamma);
    M = mean(mean(map));

    l = size(map,2);
    trd = 0.3;
    edge = [];

    for j=1:l-1
        points = find (map(:,j)< trd);
        edge(1,j) = points(1,1);
    end
    lenght(1,i) = mean(edge)
end
mean10_lenght = mean(lenght)
```

4.4 Arduino set-up

The relative movement of the ultrasound probe is detected by a laser optical sensor, connected to an Arduino board. The PixArt Imaging's PAT9125EL sensor is a miniature and low-power digital tracking chip that measures changes in position by optically acquiring sequential surface images and mathematically determines speed, direction and magnitude of motion. It is connected with the Arduino UNO board that is an open-source microcontroller based on the Microchip ATmega328P microcontroller. It has 14 Digital pins, 6 Analog pins and it is connected with the laptop via a USB cable.



Figure 4. 11 Arduino UNO board [35]

The sensor returns integer values, and each unit is equal to $20 \mu\text{m}$. Thanks to the Arduino Software (IDE), the microprocessor is configured to read the movement in the Z-axis every 5 milliseconds. The code reported below is the Java script used to program the Arduino UNO board.

```
#include <pat9125.h>

#define PAT9125_HWI2C
boolean fsensor_enabled = true;
unsigned long timer = 0;
unsigned long period = 5;

byte buf[2];
long data;

void setup(){
  fsensor_enable();
  Serial.begin(115200,SERIAL_8N1); //
}

void loop() {
  if(millis() - timer > period){
    timer = millis();
    pat9125_update_y();
    data = pat9125_y;
    Serial.println(data);
  }
}

bool fsensor_enable()
{
  int pat9125 = pat9125_init();
  fsensor_enabled = pat9125?true:false;
  return fsensor_enabled;
}

void fsensor_disable() {
  fsensor_enabled = false;
}
```

In order to acquire the relative probe movement, the sensor chip is fixed to a 3D printed structure positioned in a static position near the ultrasound probe. To acquire a better signal the sensor points th ultrasound gray structure.

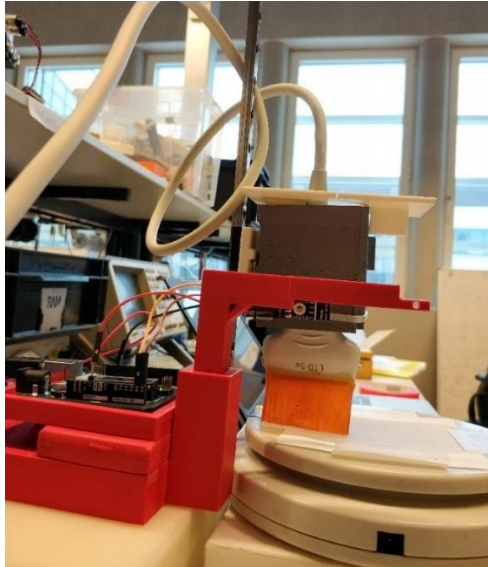


Figure 4. 12 Position of the optic sensor respect to the probe

The signal captured by the Arduino board is, then transferred to the laptop thanks to the Matlab script reported below. This script reads the Arduino board as a serial port and capture the values and save them on an external text file.

```
delete(instrfindall);

s = serial('COM3','BaudRate', 115200);
s.InputBufferSize = 4000;
fopen(s);

i=0;
dis = [];

text = fopen('sincro.txt','w');

for i=1:1000

    val = fscanf(s,'%d\n');
    dis(i) = val;
    val = val*20; %returns the value in µm
    fprintf('%d\n',dis(i));
    fprintf(text, '\n%f\r\n',dis(i));
    i= i+1;

    c(i,:) = clock;

end
```

5. RESULTS

In this chapter the results obtained are illustrated and commented. It is important to underline that the goal of these experiment is to test the use of an acoustically transparent pad and ultrasound imaging as tools to evaluate the pressure distribution on its surface. The scope is to obtain accurate elastographic measurements of tissue during an autonomous breast scanning completed by a 7-DOF KUKA arm. It is clear that elastographic measurements should be evaluated during the probe movement, and not in a static environment as it is simulated in these experiments. In this evaluation, shear forces are not considered, but clearly have a huge impact in the real case.

5.1 Experiment: Calibration

The ultrasound probe is placed on the pad. To increment the image quality, the contact surface between the probe and the pad is filled with ultrasound gel. It is composed of water and propylene glycol and fills the spaces between the ultrasound transducer and the pad, removing air bubbles and permitting to the ultrasound wave to travel with no reflection. Then, ten images are recorded; the resolution of one pixel is equal to the ratio between the depth value obtained with the ultrasound and the same length measured with a caliber. They are respectively equal to 318 pixels and 23.4 mm; thus, the resolution is:

$$\frac{\text{Lenght in mm}}{\text{number of pixels}} = \frac{23.4 \text{ mm}}{318 \text{ pixels}} = 0.0735 \text{ mm/pixel} \quad (5.1)$$

This value is fixed, and it is used for the other two experiments.

5.2 Experiment: Deformation/Weight

To roughly estimates the stress-strain relationship, the measurement of the pad depth at different pressure are evaluated. The ultrasound probe is loaded with different weights, placed on its upper surface and simultaneously ten ultrasound images are processed to estimate the depth of the pad with the methods described in Chapter 4. The number of pixels composing the pad image is multiplied for 0.0735 mm/pixel, representing the pixel resolution, and the value in mm of the depth is calculated. The external movements of the ultrasound probe are recorder by the laser sensor. However, sometimes it is not able to evaluate the movement correctly. This is probably due to the fact that the probe movement caused by

the weight is instantaneous and the sensor, that has a sampling rate of 5 ms, does not have the time resolution to detect the position variation. The values calculated are gathered in the table below:

<i>Weight [g]</i>	<i>Weight measured [g]</i>	<i>Force applied [N]</i>	<i>Pad Depth [mm]</i>	<i>Displacement Laser [mm]</i>
50	243	2.38	22.4	X
100	312	3.06	23.3	1
150	368	3.61	23.4	X
200	440	4.32	23.2	X
300	524	5.14	22.4	X
400	634	6.22	24.2	0.74
500	732	7.18	23.8	1.28
600	822	8.06	23.2	1.08
700	933	9.15	22.7	0.6
800	1010	9.91	22.3	X
900	1124	11.03	22.1	0.96
1000	1240	12.16	21.4	4.68

Table 5 Values obtained in the 2nd experiment

The relationship between the pad depth and the weight applied is showed in figure 5.1. It is possible to notice that the firsts values do not follow any reasonable trend, but after a peak value recorded at 400 g, the pad depth starts decreasing linearly with the increasing of the weight applied.

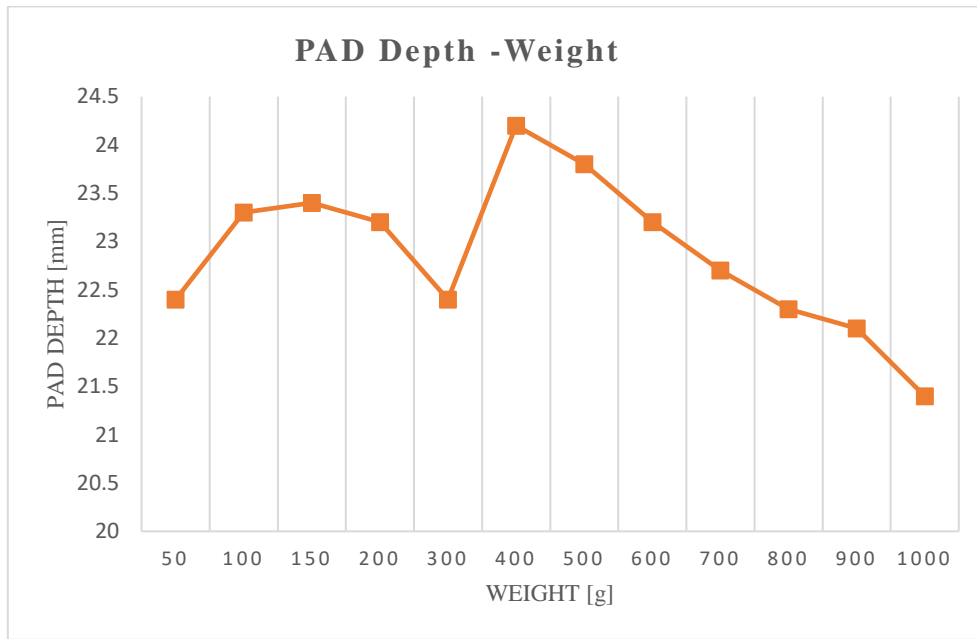


Figure 5. 1 Depth – Weight relationship

The first values are probably affected by the presence of the ultrasound gel at the contact interface between the transducer and the pad. The gel is a viscous material that change position during the initial compression and thus, affect the final results. Supposing that the presence of gel becomes negligible after a weight of 400 g, it is possible to roughly plot the stress-strain relationship of the pad detected by the ultrasound pressure sensor, during a compression operation. For a simpler visualization, strain values are reported in their absolute terms.

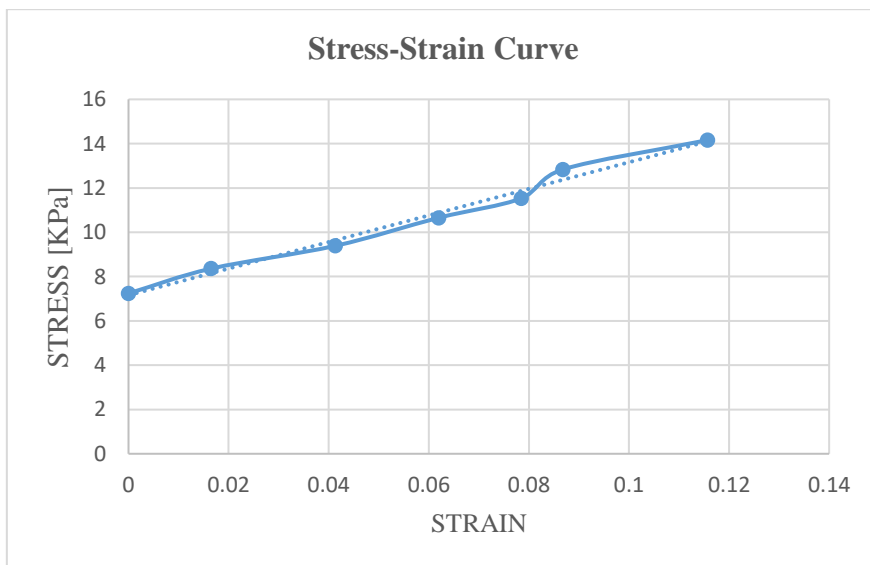


Figure 5. 2 Stress Strain curve

The curve can be fitted with a linear regression, which is characterized by a pendency of 60 KPa. This value can be roughly considered as the compressive strength of the pad material that is composed by a mixture of Plastisol, hardener and Silica gel. It is clear that this value is referred only to the referred to the presented material, but this simple evaluation can be part of the calibration process for each ultrasound pressure sensor evaluated. It is important to remark that the only compression case is evaluated, considering the pad made of a material that shows simple linear elastic properties. This represents a simplification of the real behavior of a polymer, thus more accurate studies are needed.

5.3 Experiment: Pad deformation / Probe movement

The aim of this experiment is to test if the pad deformation measured with the ultrasound sensor follows the same trend of the ultrasound probe movement. The ultrasound probe is manually pressed against the pad and the ultrasound images are gathered simultaneously with the laser sensor signal for an evaluation time of 5 seconds. To complete this task two different laptops are used, so for synchronizing the value obtained with the two modalities, the Matlab function clock is used. This function returns a six-element date vector containing the current date and time in decimal form. Figure 5.3 shows the results obtained.

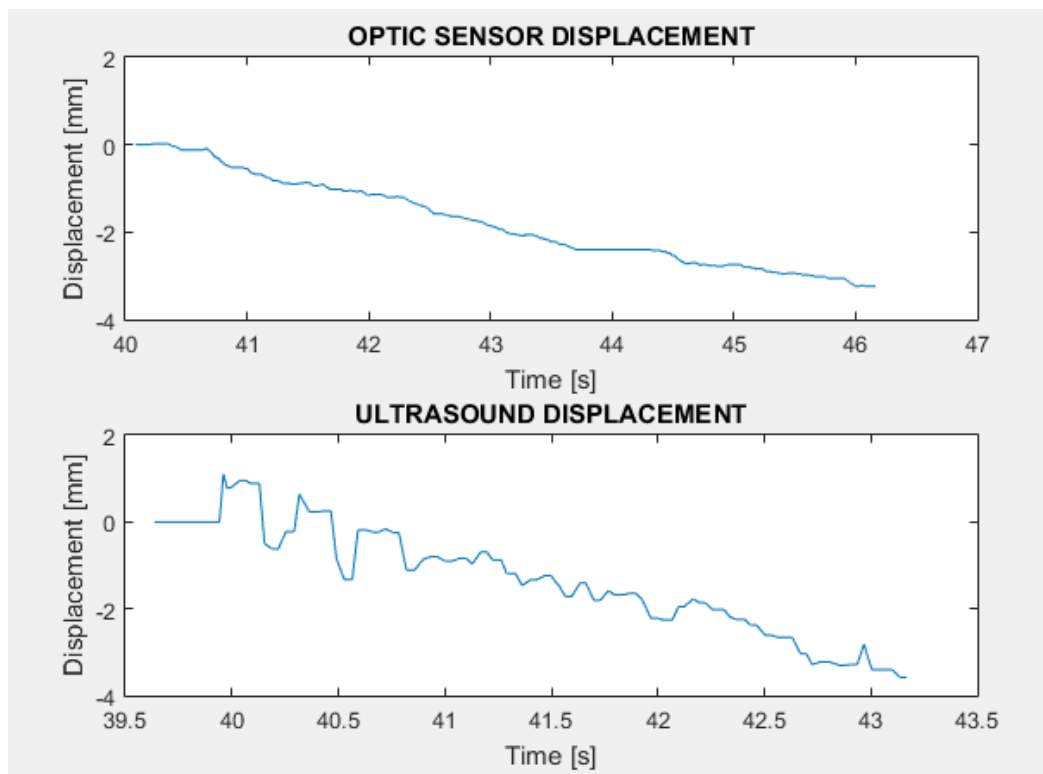


Figure 5. 3 Displacement sensed by the optic sensor and the ultrasound imaging

As it possible to notice the displacement values measured by the ultrasound pressure sensor are noisy but follow a reasonable trend. The first values are probably affected by the presence of ultrasound gel at the contact surface. The comparison graph is showed in the figure below.

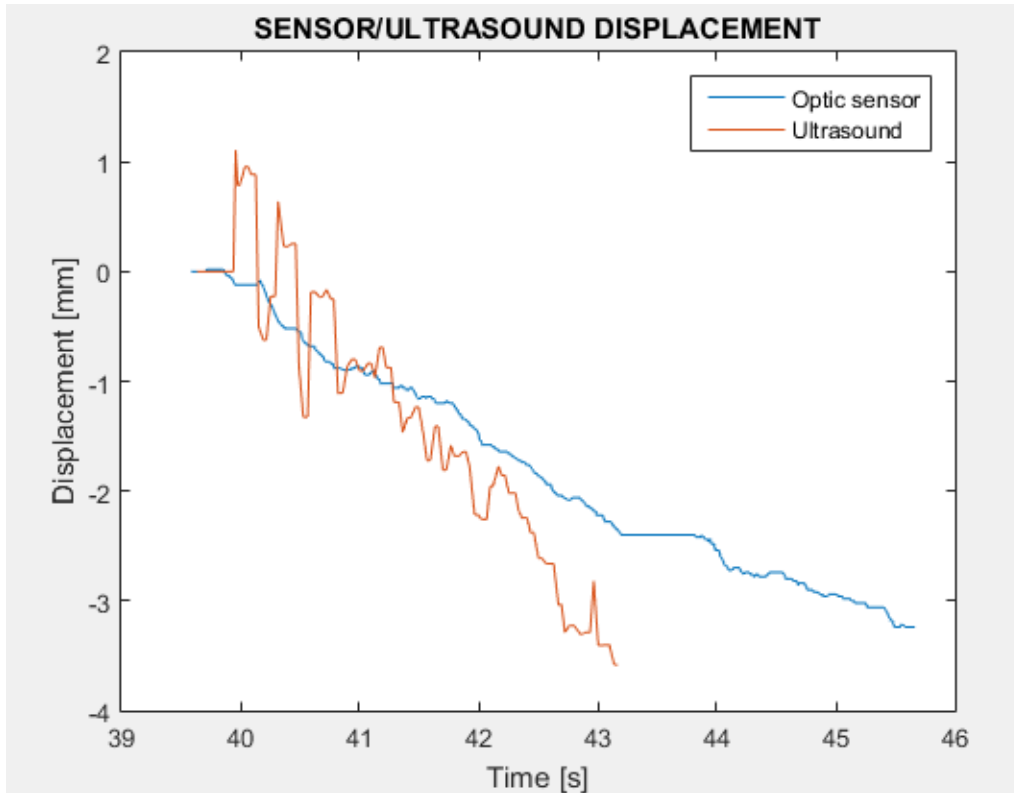


Figure 5.4 Comparison of the displacement measured simultaneously

The displacement measured with the ultrasound pressure sensor is higher than the one valued with the optic sensor. Besides the fact that ultrasound images are affected by simplifications and image artifacts, the ultrasound wave propagation inside a solid is strictly correlated to the internal structure of its particles. In a compressed material the particles are packed in a smaller volume and the distance between two particles is lower than in the uncompressed material. This fact can cause a different propagation of the sound waves and, in the specific case of the ultrasound pressure sensor evaluated, could introduce an error in the evaluation of the displacement. In fact, the displacement is found multiplying the numbers of pixel with its resolution, which is founded with a calibration process that consider an uncompressed pad. To reduce this error, a possible solution strategy could be to repeat the calibration process in different pad compression states and see if the numerical value is equal for each case. If it is not, it is possible to implement an algorithm that evaluates the displacement considering a value of resolution of pixel that change in correlation with the applied pressure.

CONCLUSIONS

The goal of this project was to design an acoustically transparent pressure sensor able to assess elastographic measurements of the breast. Two different strategies are been investigated: the use of soft tactile sensors and an implementation of a sensor technology that uses sequentially ultrasound images to detect the deformation of an acoustically transparent pad mounted on the tip of the ultrasound transducer. The idea is to obtain the value of the pressure applied to the probe, thanks to the evaluation of the deformation of the pad, made of a material characterized by a known elastic modulus. The pad is made of a controlled mixture of Plastisol, hardener and Silica gel, heated and treated in a vacuum oven and poured in a mold of a specific shape. To test the manufactured material a rectangular shape tester is made and evaluated in order to detect the interaction with the ultrasound probe and to write a code able to study autonomously its deformation. To evaluate the numerical value of the displacement, a calibration test was made to quantify the length resolution of a pixel of the ultrasound image. The resulting ultrasound pressure sensor has a sensitivity of 60 KPa and shows a linear transfer function only with values higher than 6 KPa, probably due to the presence of ultrasound gel between the tester and the ultrasound transducer, that introduce sensible errors in the correct evaluation of the pad displacement due to compression. In order to increment the sensitivity of the sensor described, a pad made of a softer material can be evaluated. However, for the intrinsic ultrasound image artifacts is clear that for a good estimation of the pad displacement, it is necessary to have a pad with a significant depth value. This leads to the fact that is not possible consider accurate a linear elastic model of the material used and shear forces cannot be ignored. Moreover, a pad with a high depth causes a substantial attenuation of the soundwaves that arrive to the tissue to detect with a low energy.

Other proven methods that assess elastographic measurement of soft tissues thanks to ultrasound detection, are strain elastography and shear wave elastography, fully described in section 1.1.2. These evaluations use the same data captured by the ultrasound transducer for a normal ultrasound image formation, so can be performed in few minutes and do not need any supplement external parts. Thus, a possible solution for breast elastographic assessment could be the implementation of an ultrasound system able to perform this evaluation.

The work is part of the MURAB project, that has the aim to improve the breast biopsy procedure using a 7-DOF KUKA robot arm that steers an ultrasound transducer along a precise scanning trajectory to gather 3D volume image and stiffness value in order to evaluate the best position for the needle insertion. The robot has an energy-based impedance controller and a visual servoing algorithm based on sequentially ultrasound images of breast. However, the intrinsic movement of the breast or the

uncontrolled movement of the patients introduce significant errors in the construction of 3D images of breast, and the control algorithm fails its evaluation. An alternative visual servoing technique is introduced in chapter 2, and it aims to implement touch sensing in robot system in order to process material characteristics and shapes of the surrounding objects. The idea proposed is to equip the ultrasound probe with a soft tactile sensor able to detect breast deformation for the implementation of the system control and simultaneously assess mechanical elastographic measurements. The information provided by the tactile sensor can be implemented with the data measured with strain elastography and assess the acousto-mechanical imaging. However, the interaction between the soundwave and the material of tactile sensors are not known, thus more studies are needed to evaluate the effective usability of this solution.

BIBLIOGRAPHY

1. Bray F, Ferlay J, Soerjomataram I, Siegel RL, Torre LA, Jemal A.
Global cancer statistics 2018: GLOBOCAN estimates of incidence and mortality worldwide for 36cancers in 185 countries
J Natl Cancer Inst. 2000
2. Bobo JK, Lee NC, Thames SF
Clinical breast examinations reported to a national screening program from 1995 through 1998
J Natl Cancer Inst. 2000
3. Bleyer A, Welch HG
Effect of three decades of screening mammography on breast-cancer incidence
N Engl J Med. 2012 Nov 2
4. Saslow D, Boetes C, Burke W, Harms S, Leach MO, Lehman CD, Morris E, Pisano E, Schnall M, Sener S, Smith RA, Warner E, Yaffe M, Andrews KS, Russell CA;
American Cancer Society guidelines for breast screening with MRI as an adjunct to mammography.
CA Cancer J Clin.
5. Lord SJ, Lei W, Craft P, Cawson JN, Morris I, Walleser S, Griffiths A, Parker S, Houssami N
A systematic review of the effectiveness of magnetic resonance imaging (MRI) as an addition to mammography and ultrasound in screening young women at high risk of breast cancer
Eur J Cancer. 2007 Sep
6. DeMartini W, Lehman C.
A review of current evidence-based clinical applications for breast magnetic resonance imaging
Top Magn Reson Imaging. 2008 June
7. Berg WA, Blume JD, Cormack JB, Mendelson EB, Lehrer D, Böhm-Vélez M, Pisano ED, Jong RA, Evans WP, Morton MJ, Mahoney MC, Larsen LH, Barr RG, Farria DM, Marques HS, Boparai K
Combined screening with ultrasound and mammography vs mammography alone in women at elevated risk of breast cancer
2008 May 14

8. Siddiqui MM, Rais-Bahrami S, Turkbey B, George AK, Rothwax J, Shakir N, Okoro C, Raskolnikov D, Parnes HL, Linehan WM, Merino MJ, Simon RM, Choyke PL, Wood BJ, Pinto PA
Comparison of MR/ultrasound fusion-guided biopsy with ultrasound-guided biopsy for the diagnosis of prostate cancer
JAMA. 2015 Jan
9. S. Luo, W. Mou, K. Althoefer and H. Liu
Localizing the object contact through matching tactile features with visual map
IEEE International Conference on Robotics and Automation (ICRA), Seattle, WA, 2015
10. Qiang Li, Carsten Schürmann, Robert Haschke, Helge Ritter
A control framework for tactile servoing
11. Sarvazyan A, Hall TJ, Urban MW, Fatemi M, Aglyamov SR, Garra BS
An Overview of elastography – an emerging branch of medical imaging
Curr Med Imaging Rev
12. Egorov V, Sarvazyan AP
Mechanical Imaging of the Breast
IEEE transactions on medical imaging. 2008
13. Egorov V, Kearney T, Pollak SB, Rohatgi C, Sarvazyan N, Airapetian S, Browning S, Sarvazyan A
Differentiation of benign and malignant breast lesions by mechanical imaging
Breast Cancer, Research and Treatment. 2009
14. B. Li, Y. Shi, A. Fontecchio and Y. Visell
Mechanical Imaging of Soft Tissues with a Highly Compliant Tactile Sensing Array
IEEE Transactions on Biomedical Engineering, March 2018
15. Thomas L. Szabo
Diagnostic Ultrasound Imaging: Inside Out
Academic Press, 21 set 2004
16. L. Odegaard, S. Holm, F. Teigen, and T. Kleveland
Acoustic field simulation for arbitrarily shaped transducers in a stratified medium
Proceedings IEEE Ultrasonics Symposium, 1994. Basic physics of ultrasound
17. Dey, Joyoni & Kuc, R.
Modeling and Analysis of Ultrasound Propagation in Layered Medium.
1999
18. Zhouye Chen.
Reconstruction of enhanced ultrasound images from compressed measurements.

- Emerging Technologies [cs.ET]. Université Paul Sabatier - Toulouse III, 2016
19. Haim Azhari
Basics of Biomedical Ultrasound for Engineers
John Wiley & Sons, Inc., 2010
20. Nimrod M. Tole,
Basic Physics of Ultrasonographic Imaging
World Health Organization
21. Sigrist RMS, Liao J, Kaffas AE, Chammas MC, Willmann JK.
Ultrasound Elastography: Review of Techniques and Clinical Applications.
Theranostics. 2017 Mar
22. Ophir J, Alam SK, Garra BS, Kallel F, Konofagou EE, Krouskop T, Merritt CR, Righetti R, Souchon R, Srinivasan S, Varghese T.
Elastography: Imaging the elastic properties of soft tissues with ultrasound.
J Med Ultrason (2001). 2002 Dec
23. A. R. Skovoroda, S. Y. Emelianov, M. A. Lubinski, A. P. Sarvazyan and M. O'Donnell
Theoretical analysis and verification of ultrasound displacement and strain imaging.
Ultrasonics, Ferroelectrics, and Frequency Control, vol. 41, no. 3, pp. 302-313, May 1994.
24. Barr RG.
The Role of Sonoelastography in Breast Lesions.
Semin Ultrasound CT MR. 2018 Feb
25. NG, Alexander; SWANEVELDER, Justiaan.
Resolution in ultrasound imaging.
Continuing Education in Anaesthesia Critical Care & Pain, 2011
26. Prabhu SJ, Kanal K, Bhargava P, Vaidya S, Dighe MK.
Ultrasound artifacts: classification, applied physics with illustrations, and imaging appearances.
Ultrasound Q. 2014 Jun
27. Quien MM, Saric M.
Ultrasound imaging artifacts: How to recognize them and how to avoid them.
Echocardiography. 2018 Sep
28. Cortela, Guillermo & Benech, Nicolás & Pereira, Wagner & Negreira, C
Characterization of Acoustical Properties of a Phantom for Soft Tissues (PVCP and Graphite Powder) in the Range 20-45°C.
Physics procedia. 2015
29. Spirou GM, Oraevsky AA, Vitkin IA, Whelan WM.
-

- Optical and acoustic properties at 1064 nm of polyvinyl chloride-plastisol for use as a tissue phantom in biomedical optoacoustics.**
Phys Med Biol. 2005 Jul
30. Cafarelli A, Verbeni A, Poliziani A, Dario P, Menciassi A, Ricotti L.
Tuning acoustic and mechanical properties of materials for ultrasound phantoms and smart substrates for cell cultures.
Acta Biomater. 2017 Feb
31. Siemens L10-5V Datasheet
<https://www.platinumhc.com/siemens-ultrasound/nx2/siemens-acuson-nx2-transducer-flyer.pdf>
32. Magewell USB Capture HDMI device
<http://www.magewell.com/products/usb-capture-hdmi-gen-2>
33. Karamalis A, Wein W, Klein T, Navab N.
Ultrasound confidence maps using random walks.
Med Image Anal. 2012 Aug
34. Stijn de Looijer (Master Thesis)
Intrinsically Passive Control for Ultrasound-guided Robotic Scanning of the Breast
Delt University of Technology, University of Twente
35. Arduino uno board
<https://store.arduino.cc/arduino-uno-rev3>
36. Y. Emelianov, Stanislav
Acousto-Mechanical Imaging for Breast Cancer Detection. 2003
37. SureTouch
<https://suretouch.global/>
38. Li, Bin & Gao, Yang & Fontecchio, Adam & Visell, Yon.
Soft capacitive tactile sensing arrays fabricated via direct filament casting.
Smart Materials and Structures. 2016
39. Yao, Shanshan & Zhu, Yong.
Wearable multifunctional sensors using printed stretchable conductors made of silver nanowires. Nanoscale. 2014
40. Saskia Nies (Bachelor Thesis)
Force sensing with an acoustically transparent pressure sensor to improve robotic assisted breast biopsy
University of Twente
-